RESEARCH PAPER

Human Vaccines & Immunotherapeutics 9:2, 283–290; February 2013; © 2012 Landes Bioscience

TLR9 adjuvants enhance immunogenicity and protective efficacy of the SE36/AHG malaria vaccine in nonhuman primate models

Takahiro Tougan,[1] Taiki Aoshi,[2,3] Cevayir Coban,[4] Yuko Katakai,[5] Chieko Kai,[6] Yasuhiro Yasutomi,[7] Ken J. Ishii[2,3,†,*] and Toshihiro Horii[1,†,*]

[1]Department of Molecular Protozoology; Research Institute for Microbial Diseases; Osaka University at Suita; Osaka, Japan; [2]Laboratory of Adjuvant Innovation; National Institute of Biomedical Innovation (NIBIO) at Ibaraki; Osaka, Japan; [3]Laboratory of Vaccine Science; Immunology Frontier Research Center (IFReC); Osaka University at Suita; Osaka, Japan; [4]Laboratory of Malaria Immunology; Immunology Frontier Research Center (IFReC); Osaka University at Suita; Osaka, Japan; [5]The Corporation for Production and Research of Laboratory Primates at Tsukuba; Ibaragi, Japan; [6]Laboratory Animal Research Center; The Institute of Medical Science; The University of Tokyo at Minato-ku; Tokyo, Japan; [7]Tsukuba Primate Research Center; National Institute of Biomedical Innovation at Tsukuba; Ibaragi, Japan

[†]These authors contributed equally to this work.

Keywords: SE36, malaria vaccine, *Plasmodium falciparum*, TLR9 ligand adjuvant, synthetic hemozoin, CpG ODN, nonhuman primate model

Abbreviations: SERA, serine repeat antigen; AHG, aluminum hydroxide gel; ODN, oligodeoxyribonucleotides; sHZ, synthetic hemozoin; GMP, good manufacturing practice

The SE36 antigen, derived from serine repeat antigen 5 (SERA5) of *Plasmodium falciparum*, is a promising blood stage malaria vaccine candidate. Ongoing clinical trials suggest the efficacy of the SE36 vaccine could be increased by the incorporation of more effective adjuvants into the vaccine formulation. In this study, we assessed the safety, immunogenicity and protective efficacy of SE36/AHG formulated with TLR9 ligand adjuvants K3 CpG oligodeoxyribonucleotides (CpG ODNs) (K3 ODN), D3 ODN or synthetic hemozoin, in two non-human primate models. SE36/AHG with or without each adjuvant was administrated to cynomolgus monkeys. A combination of TLR9 ligand adjuvant with SE36/AHG induced higher humoral and cellular immune response compared with SE36/AHG alone. Administration of a crude extract of *P. falciparum* parasite resulted in the induction of more SE36-specific IgG antibodies in monkeys vaccinated with a combination of SE36/AHG and adjuvant, as opposed to vaccination with SE36/AHG alone. The most effective TLR9 ligand, K3 ODN, was chosen for further vaccine trials in squirrel monkeys, in combination with SE36/AHG. All monkeys immunized with the combined SE36/AHG and K3 ODN formulation effectively suppressed parasitemia and symptoms of malaria following challenge infections. Furthermore, no serious adverse events were observed. Our results show that the novel vaccine formulation of K3 ODN with SE36/AHG demonstrates safety, potent immunogenicity and efficacy in nonhuman primates, and this vaccine formulation may form the basis of a more effective malaria vaccine.

Introduction

The fight against malaria is on-going across several fronts. Although progress has been made in combating malaria, there is no question that a key tool against this parasite would be an effective vaccine. As the malaria vaccine portfolio proceeds through development, an increasing number of clinical trials have confirmed the critical importance of presenting the most appropriate antigen/adjuvant in a formulation that will likely elicit the desired immune response.[1]

This was illustrated in trials of RTS,S-based vaccines where only 2/7 individuals were protected with an in oil-in water emulsion, whereas 6/7 individuals were fully protected when the antigen was formulated in this emulsion and supplemented with the immune stimulants monophosphoryl lipid A and QS21.[2] In studies using long synthetic peptides from the conserved C-terminal region of merozoite surface protein (MSP)-3 formulated with Alhydrogel, antibody titers were sustained for over a year. A biological activity of the antibodies against *P. falciparum* as determined in vitro by antibody-dependent cellular inhibition (ADCI) and in vivo by passive transfer in *P. falciparum*-infected SCID mice. In vitro, the antibodies induced an inhibition of the *P. falciparum* erythrocytic growth in a monocyte-dependent manner, which was in most instances as high as or greater than that induced by natural antibodies from immune African adults. In vivo transfer of the volunteers' sera into *P. falciparum*–infected

*Correspondence to: Ken J. Ishii and Toshihiro Horii; Email: kenishii@biken.osaka-u.ac.jp and horii@biken.osaka-u.ac.jp
Submitted: 09/03/12; Revised: 11/07/12; Accepted: 11/18/12
http://dx.doi.org/10.4161/hv.22950

humanized SCID mice profoundly reduced or abrogated parasitemia. These inhibitory effects were related to the antibody reactivity with the parasite native protein, which was seen in 60% of the volunteers, and remained in samples taken one year postimmunization.[3]

The blood-stage antigen SERA5 (for a review see ref. 4) is a promising blood-stage vaccine candidate against *P. falciparum*. SERA5 is largely produced during the late trophozoite and schizont stages.[5-7] Recombinant SE47' antigen, based on the SERA5 molecule, conferred protective immunity against parasite challenge in both *Aotus* and squirrel monkeys.[8-11] Mouse and rat antibodies against the SE47', likewise, inhibited parasite growth in vitro.[12-14] However, SE47' is highly hydrophobic, making large-scale manufacturing under good manufacturing practice (GMP) conditions a major challenge. Therefore, we constructed a new recombinant antigen, SE36, lacking the serine repeats. SE36 absorbed to the adjuvant aluminum hydroxide gel (SE36/AHG) was prepared under GMP conditions. SE36/AHG was highly immunogenic and anti-SE36 IgG titers lasted more than 1 y in chimpanzees.[15] Squirrel monkeys vaccinated with SE36/AHG were protected against high parasitemia, and serum anti-SE36 IgG titers were boosted after malaria parasite challenge. A human phase 1a clinical trial in Japan demonstrated that SE36/AHG (100 μg/1,000 μg) was safe, well-tolerated and immunogenic.[15] However, the mean titer of induced anti-SE36 antibody in the phase 1a trial was lower than that in African high responders.

Synthetic oligodeoxyribonucleotides (ODNs) containing immunostimulatory unmethylated cytosine-guanosine dinucleotides (CpG motifs) are potentially useful adjuvants and have been evaluated for veterinary and human vaccines.[16] These so-called CpG ODNs are categorized into two major classes, K- and D-type. K-type ODNs trigger the maturation of dendritic cells and stimulate the production of IgM and interleukin (IL)-6.[17,18] The D-type ODNs trigger antigen-presenting cell (APC) maturation and preferentially induce interferon (IFN)-α and -γ secretion.[18,19] It has been reported that K3 ODN effectively induces IL-6 production and cell proliferation, and that D35 ODN effectively secretes IFN-α in rhesus macaques.[20]

Another TLR9 ligand, synthetic hemozoin (sHZ, also known as β-hematin), is also a potent adjuvant for malarial antigens.[21] Hemozoin, a malaria pigment, is a detoxified product of heme molecules found in food vacuoles of the malaria parasites.[22,23] In previous studies, it was shown that purified HZ activates macrophages, thereby producing pro-inflammatory cytokines, chemokines and nitric oxide. HZ has also been shown to enhance human myeloid dendritic cell maturation.[21,24] Furthermore, the adjuvant function of sHZ was validated in a canine antiallergenic vaccine model.[25] Thus, HZ can influence adaptive immune responses to malaria infection and may have therapeutic value in vaccine adjuvant development.

We recently determined that a formulation of K3 and D35 ODNs, or sHZ with SE36/AHG was effective for the induction of anti-SE36 IgG in a rodent malaria model (Tougan et al., unpublished data). The purpose of this study was to increase the levels of induced antibody using a vaccine formulation containing TLR9 ligands as adjuvants. Here, we report the safety, immunogenicity and protective efficacy of the SE36/AHG formulation containing either K3 ODN, D35 ODN or sHZ as an adjuvant in non-human primate models.

Results

Adjuvant efficacy of TLR9 ligands to SE36/AHG. The adjuvant efficacy of K3 and D35 ODNs, and sHZ with SE36/AHG was examined. Twelve cynomolgus monkeys were randomly assigned to four groups. SE36/AHG, with or without each adjuvant, was administered four times and SE36-specific IgG titer was measured. Two weeks after the second immunization (Day 36), mean anti-SE36 antibody titers were 54.5, 432.9 ($p < 0.05$), 68.8 and 270.1 in the SE36/AHG, SE36/AHG with K3 ODN, SE36/AHG with D35 ODN and SE36/AHG with sHZ groups, respectively (**Fig. 1A and B**). Two weeks after the third immunization (Day 112), mean antibody titers were 182.2, 2258.9 ($p < 0.05$), 704.3 and 1276.1, respectively (**Fig. 1A and B**). Two weeks after the fourth immunization (Day 379), mean antibody titers were 237.8, 1960.8 ($p < 0.05$), 548.2 and 791.3 in the respective groups (**Fig. 1A and B**). At the three time points post-administration (**Fig. 1A and B**), the formulations including K3 ODN and sHZ elicited significantly higher anti-SE36 antibody titers. In particular, K3 ODN remarkably enhanced the antibody response after each administration. Furthermore, titers in individual monkeys from each group were compared immediately before each immunization to observe sustainability of the antibody titers. After the second immunization, mean antibody titers were 13.9, 176.0, 17.3 and 43.0 in the SE36/AHG, SE36/AHG with K3 ODN, SE36/AHG with D35 ODN, and SE36/AHG with sHZ groups, respectively (**Fig. 1A and B**). After the third immunization, mean antibody titers were 17.6, 157.7, 26.6 and 21.3, respectively (**Fig. 1A and B**). After the fourth immunization, mean antibody titers were 24.6, 164.5, 94.1 and 24.9 in the respective groups (**Fig. 1A and B**). These results indicate that the formulation with K3 ODN, but not sHZ, was able to sustain antibody titers although both were able to elicit statistically significant titers at each immunization time point.

Overall, the formulation of K3 ODN with SE36/AHG most effectively induced and maintained SE36-specific IgG titers. Additionally, there was no statistically significant difference between titers after the third or fourth immunization, with means of 1960.8 and 2258.9, respectively. This result suggests that an initial immunization with two boosters should be sufficient to confer the maximum levels of antibody titer (**Fig. 1A and B**).

Cytokine responses to SE36 stimulation. To examine the involvement of SE36-specific helper T cell responses, we measured cytokine secretion from peripheral blood mononuclear cells (PBMCs) 2 weeks after the second and fourth immunizations. IFN-γ was used as a marker of the Th1 response, IL-5 and IL-13 as markers of the Th2 response, and IL-17 as a marker of the Th17 response [Day 36 (i) and Day 379 (v) in **Fig. 1**]. On Day 36, IFN-γ was significantly induced in the SE36/AHG with K3 ODN group. IL-5 and IL-13 were significantly induced in each group where K3 ODN or sHZ was employed. These results suggest that a formulation containing K3 ODN promotes both Th1 and Th2 responses.

It appears that sHZ promotes the Th2 response only (**Fig. 2A**). On Day 379, IFN-γ, IL-5 and IL-13 were induced in groups containing K3 ODN in the formulation, along with the SE36/AHG and sHZ groups. These results indicate that four immunizations promote both Th1 and Th2 responses. IL-17 was induced in all four groups on Day 36, with cytokines significantly induced in SE36/AHG and sHZ groups, but only slightly induced in groups where K3 ODN and D35 ODN was included in the formulation (**Fig. 2B**). Of interest to us, the production of all cytokines was not prominent in the SE36/AHG with D35 ODN group at both time points despite the clear antibody titer induction in this group.

Immunostimulation using crude extracts of *P. falciparum*. To examine whether SE36-specific IgGs can be boosted by natural SERA5 antigen exposure after natural infection, we injected a crude extract of *P. falciparum* strain 3D7 into cynomolgus monkeys to mimic the complex mixture of *Plasmodium* antigens encountered during natural infection. The crude extract was administered at Day 583 (**Fig. 1**) and SE36-specific IgG titers were measured at 0 (Day 583), 1 and 2 weeks after injection. Although there was no statistical difference between week 1 and 2, in all groups, SE36-specific IgG titers were enhanced after injection (**Fig. 3**). We, thus, speculate that SE36-specific IgG antibodies could be boosted by malaria infection.

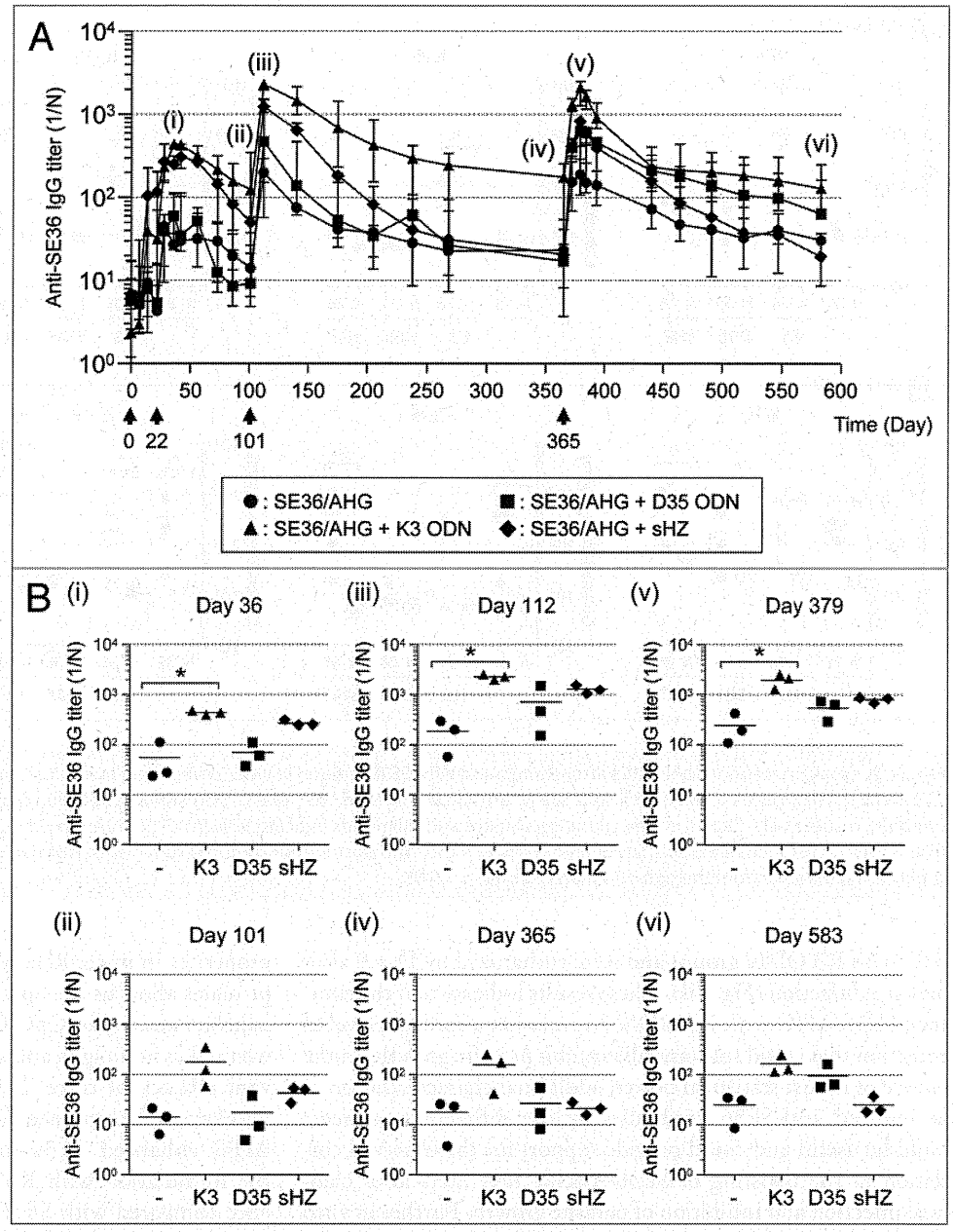

Figure 1. Formulation with K3 ODN effectively enhances SE36-specific IgG titers. (**A**) Time-course of SE36-specific IgG antibody titer. Cynomolgus monkeys were administered the same dose on days 0, 22, 101 and 365 (arrows). Sera were collected on days 0, 7, 14, 22, 28, 36, 42, 56, 73, 86, 101, 112, 140, 175, 205, 238, 268, 365, 372, 379, 384, 393, 440, 464, 491, 518, 547 and 583. Closed circles, triangles, squares and diamonds show the median titers (n = 3/group) of SE36/AHG, SE36/AHG with K3 ODN, SE36/AHG with D35 ODN and SE36/AHG with sHZ, respectively. Ranges are shown by bars. (**B**) Titers for individual monkeys subjected to different treatments on days 36 (i), 101 (ii), 112 (iii), 365 (iv), 379 (v) and 583 (vi) are compared. Statistical analysis for four groups was performed using non-parametric ANOVA (Kruskal-Wallis) with Dunn's post-hoc test; * indicates significant difference, $p < 0.05$.

Vaccine trial in squirrel monkeys. To examine whether the formulation containing K3 ODN provided protective immunity against *P. falciparum* or not, a challenge experiment using squirrel monkeys was performed. At nine weeks after the first administration of the vaccine, blood-stage malaria challenge was done by intravenous injection of 5×10^8 infected red blood cells. It is worth mentioning that the formulation containing K3 ODN did not result in significantly higher antibody titers, which differed from the results we observed in cynomolgus monkeys (**Fig. 4A**).

All three monkeys immunized with SE36/AHG combined with K3 ODN, and one monkey immunized with SE36/AHG alone developed less than 30% parasitemia (maximum parasitemia: 22.6%, 26.8% and 13.3% in the SE36/AHG with K3 ODN group; and 22.0% in the SE36/AHG group). One monkey immunized with SE36/AHG, and two monkeys immunized with AHG combined with K3 ODN experienced fulminant infections of 40–50% parasitemia (maximum parasitemia: 42.3% in the SE36/AHG group and 47.6% and 47.8% in the

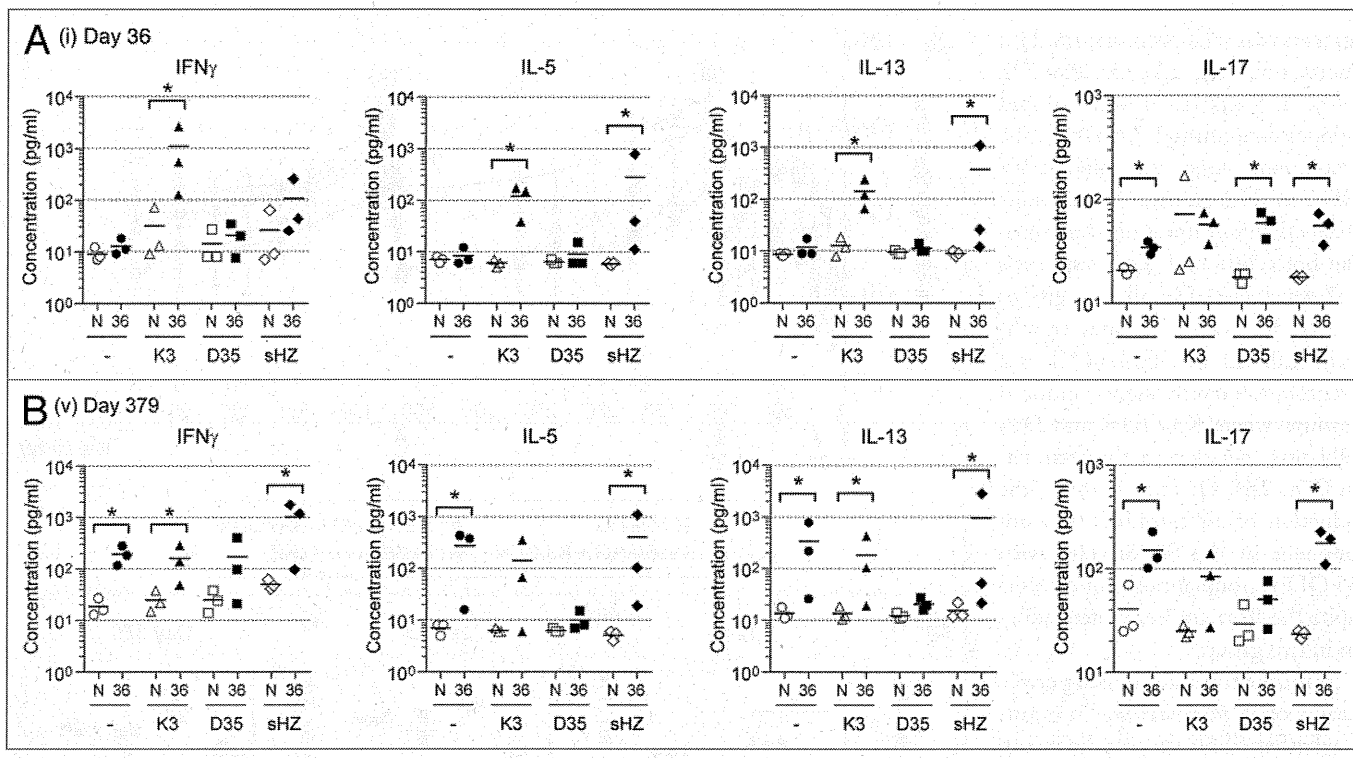

Figure 2. Cytokine response of PBMCs after stimulation with SE36 antigen in vitro. Levels in an individual cynomolgus monkey's cytokine (IFN-γ, IL-5, IL13 and IL-17) responses on days 36 (i) and 379 (v) are shown. "N" and "36" refer to non-stimulated (open symbols), and stimulated with SE36 (closed symbols), respectively. Closed circles, triangles, squares and diamonds indicate SE36/AHG, SE36/AHG with K3 ODN, SE36/AHG with D35 ODN and SE36/AHG with sHZ, respectively. Statistical analysis between pre- and post-immunization serum was performed using a Mann-Whitney U test. * indicates significant difference from the non-stimulated group, $p < 0.05$.

AHG with K3 ODN group) and were euthanized by Day 9 after challenge infection (**Fig. 4B**). These results indicate that the combined SE36/AHG with K3 ODN formulation afforded a level of protection that could substantially inhibit parasite growth. In the absence of robust statistical power, additional characterization of the induced anti-SE36 antibodies by the different treatments would be useful and could provide support for the observed correlation in the boosting of SE36-specific IgG titers after challenge infection and inhibition of parasite growth. Further in vitro assays would need to be incorporated in future studies.

To observe the importance of the anti-SE36 IgG antibody response, IgG titers against whole malaria parasite antigens were measured. For this purpose IgG titers against crude extract were measured after challenge infection. The IgG titers were immediately enhanced in all monkeys after challenge infection in contrast to responses of the anti-SE36 IgG titers (Tougan et al., unpublished data).

No serious adverse events during the studies were observed in both cynomolgus and squirrel monkeys. Common adverse reactions related to K3 ODN, such as erythema, swelling, induration or pruritus, were rarely detected at administration sites.

Discussion

Immunostimulatory CpG ODNs and sHZ that effect human immune cells in vitro often have limited immune-activating properties in mice. Relevant animal models such as non-human primates allow us the opportunity to demonstrate the safety and adjuvant activity of CpG ODNs and sHZ in vivo. In this study, we used cynomolgus and squirrel monkeys to evaluate the adjuvant efficacy of three TLR9 ligand adjuvants. In cynomolgus monkeys, all combined formulations of adjuvants with SE36/AHG enhanced SE36-specific IgG responses. In particular, the formulation with K3 ODN elicited over a 10-fold difference compared with SE36/AHG alone (**Fig. 1**). In **Figure 2**, it appears that formulations with K3 ODN enhanced the functions of helper T cells compared with those observed for SE36/AHG alone.

To date, many studies have demonstrated that various cytokines modulate an immune response during malaria infection. An increase in pro-inflammatory Th1 cytokines, such as IFN-γ and IL-12, during the acute phase of uncomplicated falciparum malaria has been inferred to play roles that contribute to an early and effective immune response, limiting progression toward a more severe course of malaria in humans.[26] Vaccine formulations containing CpG ODNs predominantly enhance Th1-associated cytokines, but Th2 responses involving IL-4 and IL-13 are often associated with AHG in mice.[16,27-30] However, the influence of CpG ODNs on cytokine responses in non-human primates has not been well characterized. In the current study, it was observed that the SE36/AHG formulation containing K3 ODN induced mixed Th1/Th2 responses in cynomolgus monkeys (**Fig. 2**).

The possibility of fluctuating T cell responses during this vaccination period is not clear as we did not perform cytokine assays on Days 112 (iii), 101 (ii), 365 (iv) or 583 (vi). Although this limitation would need to be addressed in future studies, this phenomenon has also been reported in several malaria vaccine candidates in mice, including AMA1-C1/AHG formulated with CPG 7909.[31] and SPf66-loaded PLGA microparticles.[32] A vaccination boost with recombinant SERA protein was also shown to markedly increase serum antibody titers in mice that were previously immunized with SERA plasmid DNA by gene gun vaccination.[33] In a murine malaria vaccine model, administration of *P. yoelii* $MSP1_{19}$/AHG formulated with CPG 7909, which is K-type CpG, induced a mixed Th1/Th2 response that resulted in enhanced vaccine efficacy, suggesting that the mixed Th1/Th2 response confers protective immunity against blood-stage infection.[34]

SE36-specific IgG titers were generally enhanced in all individual monkeys after injection of crude extract (**Fig. 3**). SE36 recombinant protein is derived from the N-terminal region of SERA5 based on the Honduras-1 strain corresponding to amino acids 17–382 where the serine repeats were removed (deletion of amino acids 193–225).[15] Although increased anti-SE36 IgG titers among all groups were not statistically different (**Fig. 3**), from squirrel monkey trials the formulation of K3 ODN appears effective for growth inhibition in various strains (**Fig. 4**).

In squirrel monkeys, the formulation with K3 ODN did not result in a higher antibody titer compared with the original SE36/AHG formulation, although protection that correlates with decreased parasite density in *P. falciparum* challenge was observed (**Fig. 4A and B**). The measurement of various cytokines in squirrel monkeys is not a sufficient measure of efficacy because they exhibit low levels of cross-reactivity with human cytokines.[35] Therefore, the interpretation of protective efficacy against malaria growth in terms of immunological responses is currently limited. Because the squirrel monkey is a valuable animal model for malaria vaccine development, the establishment of immunological analysis systems must provide more robust information for understanding the correlation between protective immunity and malaria infection.

No serious adverse events during the studies were observed in both cynomolgus and squirrel monkeys. Common adverse reactions related to K3 ODN were rarely detected at administration sites. Although empirical, the K3 ODN adjuvant formulation exhibited an adequate safety profile, justifying further studies to evaluate humoral and cellular responses in humans. A number of clinical trials looking at CpG ODN formulations have been initiated in the field of malaria vaccine development. Formulations of K-type ODN, CpG 7909, with MSP1 and AMA1 effectively boost antigen-specific IgG levels and demonstrate an adequate safety profile.[36-39] In clinical trials for hepatitis B (Engerix-B) and flu (Fluarix) vaccines, enhanced safety and immunogenicity of CpG 7909 formulations have been reported.[40,41]

In conclusion, our study demonstrates that the formulation of K3 ODN with SE36/AHG can result in the improvement of immune response.

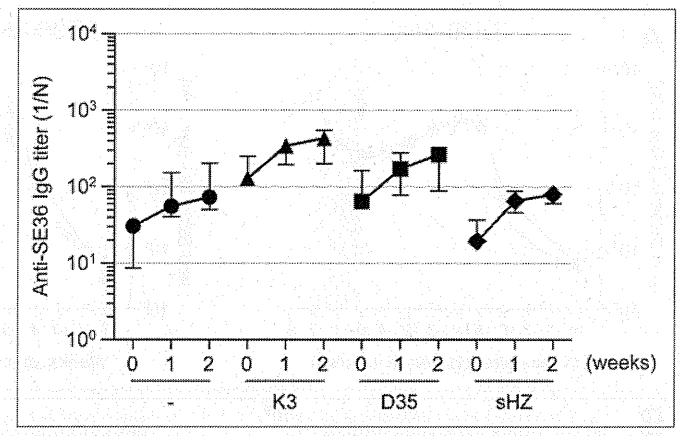

Figure 3. Trends in SE36-specific IgG antibody titers from cynomolgus monkeys after the mimic challenge infection. Crude extract was administered on day 583, and sera from each monkey were collected on day 583 (week 0), weeks 1 and 2. Median titers are represented by closed circles (SE36/AHG), triangles (SE36/AHG with K3 ODN), squares (SE36/AHG with D35 ODN) and diamonds (SE36/AHG with sHZ). Ranges are shown by bars. Statistical analysis at each timepoints (week 1 and 2) was performed using non-parametric ANOVA (Kruskal-Wallis) with Dunn's post-hoc test.

Materials and Methods

Animals, immunization and infection. A total of 12 cynomolgus monkeys (*Macaca fascicularis*) were obtained from Tsukuba Primate Research Center (TPRC), National Institute of Biomedical Innovation (NIBIO) and randomly assigned to four groups (n = 3/group). Animals were immunized subcutaneously on days 0, 22, 101 and 365 of our study with a mixture of 10 μg of SE36 and 125 μg of AHG with and without 500 μg of K3 ODN or D35 ODN in a total volume of 1 ml, or with 1.5 mM sHZ in a total volume of 1 ml. The SE36 antigen and AHG adjuvant were GMP-quality[15] and K3 and D35 ODNs and sHZ adjuvants were prepared specifically for this study. K3 and D35 were prepared as GMP quality by Gene Design Inc. and sHZ was prepared under sterile conditions with non-detectable endotoxin levels determined by LAL assay.

A total of seven squirrel monkeys (*Saimiri sciureus*) were purchased from PETSUN Co., Ltd. and randomly assigned to three groups: SE36/AHG (n = 2); SE36/AHG with K3 ODN (n = 3); and AHG with K3 ODN group (n = 2). These animals were subcutaneously immunized twice at a 3-week interval with a combination of 10 μg of SE36, 125 μg of AHG with or without 500 μg of K3 ODN in a total volume of 0.5 ml. The monkeys were splenectomized before inoculation. Nine weeks after the first immunization, parasite challenge experiments were done using the live IPC/Ray strain[42] (5×10^8 infected red blood cells) introduced intravenously in the saphenous vein. Parasitemia was monitored daily by counting 5,000 RBCs in Giemsa-stained thin blood smears. Drug treatment was commenced at Day 14, and in cases where parasitemia surpassed the set threshold parasitemia (40%) during the experimental period, the animal was euthanized to avoid sequelae, such as severe malaria, in accordance with the guidelines for animal welfare and care (Guidelines

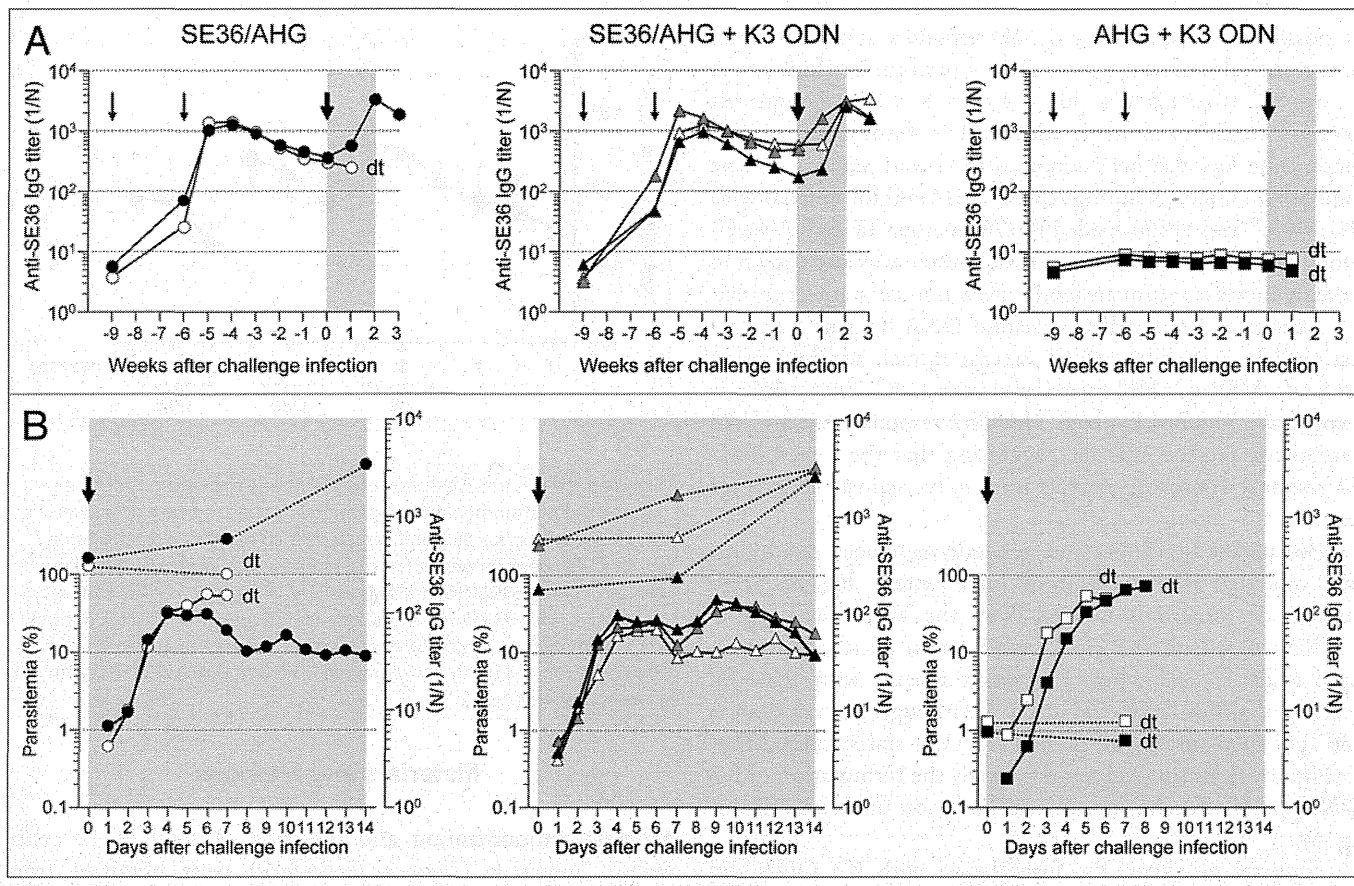

Figure 4. Vaccine trial in squirrel monkeys. (**A**) Time-course analysis of SE36-specific IgG antibody titer. Animals were administered 10 μg of SE36, 100 μg of AHG and/or 500 μg of K3 ODN at 6 and 9 weeks (thin arrows) before the challenge infection (bold arrow). (**B**) Time-course analysis of parasitemia. Parasite densities were measured up to 14 d after infection. Left Y-axis shows parasitemia and right Y-axis shows SE36-specific IgG antibody titers. Bold arrow shows the challenge infection. Dotted lines show the SE36-specific IgG antibody titers as in (**A**). In (**A**) and (**B**), light gray area shows duration of parasitemia measurement. The term "dt" denotes a monkey that was euthanized, or died owing to acute conditions. Groups are represented by closed circles (SE36/AHG), triangles (SE36/AHG with K3 ODN) and squares (AHG with K3 ODN). Black, gray and white symbols indicate the individual animals in each group.

for the Animal Care and Management of TPRC, NIBIO). All experimental protocols were approved by the Animal Welfare and Animal Care Committee at TPRC, NIBIO where animals were housed and handled. The vaccination schedule was identical to GLP studies and clinical trials for SE36 malaria vaccine.[15]

All experimental protocols were approved by the Animal Welfare and Animal Care Committee at TPRC, NIBIO. All animals were housed and handled in accordance with the Guidelines for Laboratory Animals at TPRC, NIBIO.

Adjuvants. The following human-type CpG ODNs were used: K3 ODN (ATCGACTCTCGAGCGTTCTC) and D35 ODN (GGtgcatcgatgcaggggGG). Bases shown in uppercase are phosphorothioate, and those in lowercase are phosphodiester, with CpG dinucleotides underlined.[20] These ODNs were purchased from GeneDesign Inc. The sHZ was purified from hemin chloride using the acid-catalyzed method to produce smaller and homogenous crystals as previously described.[24,25,43,44]

Antibody detection by indirect enzyme-linked immunosorbent assay (ELISA). An optimized concentration (1 μg/ml) of the recombinant SE36 antigen in carbonate/bi-carbonate buffer (pH 9.6) was used to coat wells of a 96-well MaxiSorp NUNC-Immuno plate (Nunc, Catalog number: 442404) overnight at 4°C. Plates were washed and blocked with 5% skim milk in phosphate-buffered saline (PBS) containing 0.05% Tween 20 for 2 h at room temperature. Cynomolgus monkey IgG was detected using horseradish peroxidase (HRP)-conjugated anti-monkey IgG (whole molecule) antibody produced in rabbit (Sigma-Aldrich, Catalog number: A2054). Squirrel monkey IgG was detected using anti-squirrel monkey IgG polyclonal antibody produced in rat (a kind gift from Dr. T. Tachibana) and HRP-conjugated anti-rat IgG (whole molecule) antibody produced in rabbit (Sigma-Aldrich, Catalog number: A5795). Color was developed using a TMB microwell peroxidase substrate (KPL, Catalog number: 50–76–00). The reaction was stopped with 1 M H_2SO_4. Absorbance was measured at 450/540 nm within 30 min using a SpectraMax 340PC^{384} Microplate Reader (Molecular Devices).

Detection of Cytokines. PBMCs of cynomolgus monkeys were purified by Ficoll-Hypaque (GE Healthcare, Catalog number: 17–1440–02) gradient centrifugation from blood samples obtained at days 36 and 378. Isolated cells were stimulated with GMP-quality SE36 antigen or PBS at 37°C for 24 h. Cytokine

concentrations in the culture supernatant were determined using a Milliplex Non-Human Primate Cytokine Panel - Premixed 23 Plex (Millipore, Catalog number: MPXPRCYTO40KPX23).

Immunostimulation using crude extracts of *P. falciparum*. All cynomolgus monkeys were subcutaneously injected on Day 583 with 100 μl of crude 3D7 parasite lysate (21.5 mg/ml). Blood samples were drawn at 0 (Day 583), 1 and 2 weeks later and the amount of SE36-specific IgG antibodies measured by ELISA.

Statistical analysis. Comparisons of IgG titer data among groups of monkeys were performed by non-parametric ANOVA (Kruskal-Wallis) with Dunn's post-hoc test. Comparisons of cytokine levels between two groups were performed by non-parametric Mann-Whitney U test. Statistical analyses were performed using the Graphpad Prism 5 software package.

Disclosure of Potential Conflicts of Interest

T.T., K.J.I. and T.H. hold patent for production of BK-SE36/CpG.

Acknowledgments

We thank Dr. Taro Tachibana at Department of Bioengineering, Graduate School of Engineering, Osaka City University for anti-squirrel monkey IgG antibody. This work was supported by the New Energy and Industrial Technology Development Organization (NEDO) of Japan (97S08–011 to T.H.). This work was also supported by a grant from the Cooperative Link of Unique Science and Technology for Economy Revitalization (CLUSTER) promoted by the Ministry of Education, Culture, Sports and Technology (to T.H. and K.J.I.). And this work was partially supported by Grant-in-Aid for Young Scientists (B) (22700455) from the Japanese Ministry of Education, Science, Sports, Culture and Technology (to T.T.).

References

1. Coler RN, Carter D, Friede M, Reed SG. Adjuvants for malaria vaccines. Parasite Immunol 2009; 31:520-8; PMID:19691556; http://dx.doi.org/10.1111/j.1365-3024.2009.01142.x.
2. Stoute JA, Slaoui M, Heppner DG, Momin P, Kester KE, Desmons P, et al. A preliminary evaluation of a recombinant circumsporozoite protein vaccine against Plasmodium falciparum malaria. RTS,S Malaria Vaccine Evaluation Group. N Engl J Med 1997; 336:86-91; PMID:8988885; http://dx.doi.org/10.1056/NEJM199701093360202.
3. Druilhe P, Spertini F, Soesoe D, Corradin G, Mejia P, Singh S, et al. A malaria vaccine that elicits in humans antibodies able to kill Plasmodium falciparum. PLoS Med 2005; 2:e344; PMID:16262450; http://dx.doi.org/10.1371/journal.pmed.0020344.
4. Palacpac NM, Arisue N, Tougan T, Ishii KJ, Horii T. Plasmodium falciparum serine repeat antigen 5 (SE36) as a malaria vaccine candidate.Vaccine 2011; 29:5837-45; PMID:21718740; http://dx.doi.org/10.1016/j.vaccine.2011.06.052.
5. Bzik DJ, Li WB, Horii T, Inselburg J. Amino acid sequence of the serine-repeat antigen (SERA) of Plasmodium falciparum determined from cloned cDNA. Mol Biochem Parasitol 1988; 30:279-88; PMID:2847041; http://dx.doi.org/10.1016/0166-6851(88)90097-7.
6. Delplace P, Fortier B, Tronchin G, Dubremetz JF, Vernes A. Localization, biosynthesis, processing and isolation of a major 126 kDa antigen of the parasitophorous vacuole of Plasmodium falciparum. Mol Biochem Parasitol 1987; 23:193-201; PMID:3299083; http://dx.doi.org/10.1016/0166-6851(87)90026-0.
7. Fox BA, Bzik DJ. Analysis of stage-specific transcripts of the Plasmodium falciparum serine repeat antigen (SERA) gene and transcription from the SERA locus. Mol Biochem Parasitol 1994; 68:133-44; PMID:7891737; http://dx.doi.org/10.1016/0166-6851(94)00162-6.
8. Inselburg J, Bathurst IC, Kansopon J, Barchfeld GL, Barr PJ, Rossan RN. Protective immunity induced in Aotus monkeys by a recombinant SERA protein of Plasmodium falciparum: adjuvant effects on induction of protective immunity. Infect Immun 1993; 61:2041-7; PMID:8478092.
9. Inselburg J, Bathurst IC, Kansopon J, Barr PJ, Rossan R. Protective immunity induced in Aotus monkeys by a recombinant SERA protein of Plasmodium falciparum: further studies using SERA 1 and MF75.2 adjuvant. Infect Immun 1993; 61:2048-52; PMID:8478093.
10. Inselburg J, Bzik DJ, Li WB, Green KM, Kansopon J, Hahm BK, et al. Protective immunity induced in Aotus monkeys by recombinant SERA proteins of Plasmodium falciparum. Infect Immun 1991; 59:1247-50; PMID:1900809.
11. Suzue K, Ito M, Matsumoto Y, Tanioka Y, Horii T. Protective immunity induced in squirrel monkeys with recombinant serine repeat antigen (SERA) of Plasmodium falciparum. Parasitol Int 1997; 46:17-25; http://dx.doi.org/10.1016/S1383-5769(97)00004-4.
12. Pang XL, Mitamura T, Horii T. Antibodies reactive with the N-terminal domain of Plasmodium falciparum serine repeat antigen inhibit cell proliferation by agglutinating merozoites and schizonts. Infect Immun 1999; 67:1821-7; PMID:10085023.
13. Sugiyama T, Suzue K, Okamoto M, Inselburg J, Tai K, Horii T. Production of recombinant SERA proteins of Plasmodium falciparum in Escherichia coli by using synthetic genes. Vaccine 1996; 14:1069-76; PMID:8879104; http://dx.doi.org/10.1016/0264-410X(95)00238-V.
14. Fox BA, Xing-Li P, Suzue K, Horii T, Bzik DJ. Plasmodium falciparum: an epitope within a highly conserved region of the 47-kDa amino-terminal domain of the serine repeat antigen is a target of parasite-inhibitory antibodies. Exp Parasitol 1997; 85:121-34; PMID:9030663; http://dx.doi.org/10.1006/expr.1996.4118.
15. Horii T, Shirai H, Jie L, Ishii KJ, Palacpac NQ, Tougan T, et al. Evidences of protection against blood-stage infection of Plasmodium falciparum by the novel protein vaccine SE36. Parasitol Int 2010; 59:380-6; PMID:20493274; http://dx.doi.org/10.1016/j.parint.2010.05.002.
16. Klinman DM, Klaschik S, Sato T, Tross D. CpG oligonucleotides as adjuvants for vaccines targeting infectious diseases. Adv Drug Deliv Rev 2009; 61:248-55; PMID:19272313; http://dx.doi.org/10.1016/j.addr.2008.12.012.
17. Kadowaki N, Antonenko S, Liu YJ. Distinct CpG DNA and polyinosinic-polycytidylic acid double-stranded RNA, respectively, stimulate CD11c- type 2 dendritic cell precursors and CD11c+ dendritic cells to produce type I IFN. J Immunol 2001; 166:2291-5; PMID:11160284.
18. Verthelyi D, Ishii KJ, Gursel M, Takeshita F, Klinman DM. Human peripheral blood cells differentially recognize and respond to two distinct CPG motifs. J Immunol 2001; 166:2372-7; PMID:11160295.
19. Krug A, Rothenfusser S, Hornung V, Jahrsdörfer B, Blackwell S, Ballas ZK, et al. Identification of CpG oligonucleotide sequences with high induction of IFN-alpha/beta in plasmacytoid dendritic cells. Eur J Immunol 2001; 31:2154-63; PMID:11449369; http://dx.doi.org/10.1002/1521-4141(200107)31:7<2154::AID-IMMU2154>3.0.CO;2-U.
20. Verthelyi D, Kenney RT, Seder RA, Gam AA, Friedag B, Klinman DM. CpG oligodeoxynucleotides as vaccine adjuvants in primates. J Immunol 2002; 168:1659-63; PMID:11823494.
21. Coban C, Ishii KJ, Sullivan DJ, Kumar N. Purified malaria pigment (hemozoin) enhances dendritic cell maturation and modulates the isotype of antibodies induced by a DNA vaccine. Infect Immun 2002; 70:3939-43; PMID:12065539; http://dx.doi.org/10.1128/IAI.70.7.3939-3943.2002.
22. Arese P, Schwarzer E. Malarial pigment (haemozoin): a very active 'inert' substance. Ann Trop Med Parasitol 1997; 91:501-16; PMID:9329987; http://dx.doi.org/10.1080/00034989760879.
23. Sullivan DJ. Theories on malarial pigment formation and quinoline action. Int J Parasitol 2002; 32:1645-53; PMID:12435449; http://dx.doi.org/10.1016/S0020-7519(02)00193-5.
24. Coban C, Ishii KJ, Kawai T, Hemmi H, Sato S, Uematsu S, et al. Toll-like receptor 9 mediates innate immune activation by the malaria pigment hemozoin. J Exp Med 2005; 201:19-25; PMID:15630134; http://dx.doi.org/10.1084/jem.20041836.
25. Coban C, Igari Y, Yagi M, Reimer T, Koyama S, Aoshi T, et al. Immunogenicity of whole-parasite vaccines against Plasmodium falciparum involves malarial hemozoin and host TLR9. Cell Host Microbe 2010; 7:50-61; PMID:20114028; http://dx.doi.org/10.1016/j.chom.2009.12.003.
26. Torre D, Speranza F, Giola M, Matteelli A, Tambini R, Biondi G. Role of Th1 and Th2 cytokines in immune response to uncomplicated Plasmodium falciparum malaria. Clin Diagn Lab Immunol 2002; 9:348-51; PMID:11874876.
27. Chu RS, Targoni OS, Krieg AM, Lehmann PV, Harding CV. CpG oligodeoxynucleotides act as adjuvants that switch on T helper 1 (Th1) immunity. J Exp Med 1997; 186:1623-31; PMID:9362523; http://dx.doi.org/10.1084/jem.186.10.1623.
28. Jegerlehner A, Maurer P, Bessa J, Hinton HJ, Kopf M, Bachmann MF. TLR9 signaling in B cells determines class switch recombination to IgG2a. J Immunol 2007; 178:2415-20; PMID:17277148.

29. Klinman DM, Yi AK, Beaucage SL, Conover J, Krieg AM. CpG motifs present in bacteria DNA rapidly induce lymphocytes to secrete interleukin 6, interleukin 12, and interferon gamma. Proc Natl Acad Sci U S A 1996; 93:2879-83; PMID:8610135; http://dx.doi.org/10.1073/pnas.93.7.2879.
30. Lin L, Gerth AJ, Peng SL. CpG DNA redirects class-switching towards "Th1-like" Ig isotype production via TLR9 and MyD88. Eur J Immunol 2004; 34:1483-7; PMID:15114682; http://dx.doi.org/10.1002/eji.200324736.
31. Mullen GE, Giersing BK, Ajose-Popoola O, Davis HL, Kothe C, Zhou H, et al. Enhancement of functional antibody responses to AMA1-C1/Alhydrogel, a Plasmodium falciparum malaria vaccine, with CpG oligodeoxynucleotide. Vaccine 2006; 24:2497-505; PMID:16434128; http://dx.doi.org/10.1016/j.vaccine.2005.12.034.
32. Carcaboso AM, Hernández RM, Igartua M, Rosas JE, Patarroyo ME, Pedraz JL. Potent, long lasting systemic antibody levels and mixed Th1/Th2 immune response after nasal immunization with malaria antigen loaded PLGA microparticles. Vaccine 2004; 22:1423-32; PMID:15063565; http://dx.doi.org/10.1016/j.vaccine.2003.10.020.
33. Belperron AA, Feltquate D, Fox BA, Horii T, Bzik DJ. Immune responses induced by gene gun or intramuscular injection of DNA vaccines that express immunogenic regions of the serine repeat antigen from Plasmodium falciparum. Infect Immun 1999; 67:5163-9; PMID:10496891.
34. Near KA, Stowers AW, Jankovic D, Kaslow DC. Improved immunogenicity and efficacy of the recombinant 19-kilodalton merozoite surface protein 1 by the addition of oligodeoxynucleotide and aluminum hydroxide gel in a murine malaria vaccine model. Infect Immun 2002; 70:692-701; PMID:11796601; http://dx.doi.org/10.1128/IAI.70.2.692-701.2002.
35. Ozwara H, Niphuis H, Buijs L, Jonker M, Heeney JL, Bambra CS, et al. Flow cytometric analysis on reactivity of human T lymphocyte-specific and cytokine-receptor-specific antibodies with peripheral blood mononuclear cells of chimpanzee (Pan troglodytes), rhesus macaque (Macaca mulatta), and squirrel monkey (Saimiri sciureus). J Med Primatol 1997; 26:164-71; PMID:9379483; http://dx.doi.org/10.1111/j.1600-0684.1997.tb00048.x.
36. Ellis RD, Martin LB, Shaffer D, Long CA, Miura K, Fay MP, et al. Phase 1 trial of the Plasmodium falciparum blood stage vaccine MSP1(42)-C1/Alhydrogel with and without CPG 7909 in malaria naïve adults. PLoS One 2010; 5:e8787; PMID:20107498; http://dx.doi.org/10.1371/journal.pone.0008787.
37. Ellis RD, Mullen GE, Pierce M, Martin LB, Miura K, Fay MP, et al. A Phase 1 study of the blood-stage malaria vaccine candidate AMA1-C1/Alhydrogel with CPG 7909, using two different formulations and dosing intervals. Vaccine 2009; 27:4104-9; PMID:19410624; http://dx.doi.org/10.1016/j.vaccine.2009.04.077.
38. Mullen GE, Ellis RD, Miura K, Malkin E, Nolan C, Hay M, et al. Phase 1 trial of AMA1-C1/Alhydrogel plus CPG 7909: an asexual blood-stage vaccine for Plasmodium falciparum malaria. PLoS One 2008; 3:e2940; PMID:18698359; http://dx.doi.org/10.1371/journal.pone.0002940.
39. Sagara I, Ellis RD, Dicko A, Niambele MB, Kamate B, Guindo O, et al. A randomized and controlled Phase 1 study of the safety and immunogenicity of the AMA1-C1/Alhydrogel + CPG 7909 vaccine for Plasmodium falciparum malaria in semi-immune Malian adults. Vaccine 2009; 27:7292-8; PMID:19874925; http://dx.doi.org/10.1016/j.vaccine.2009.10.087.
40. Cooper CL, Davis HL, Morris ML, Efler SM, Adhami MA, Krieg AM, et al. CPG 7909, an immunostimulatory TLR9 agonist oligodeoxynucleotide, as adjuvant to Engerix-B HBV vaccine in healthy adults: a double-blind phase I/II study. J Clin Immunol 2004; 24:693-701; PMID:15622454; http://dx.doi.org/10.1007/s10875-004-6244-3.
41. Cooper CL, Davis HL, Morris ML, Efler SM, Krieg AM, Li Y, et al. Safety and immunogenicity of CPG 7909 injection as an adjuvant to Fluarix influenza vaccine. Vaccine 2004; 22:3136-43; PMID:15297066; http://dx.doi.org/10.1016/j.vaccine.2004.01.058.
42. Groux H, Perraut R, Garraud O, Poingt JP, Gysin J. Functional characterization of the antibody-mediated protection against blood stages of Plasmodium falciparum in the monkey Saimiri sciureus. Eur J Immunol 1990; 20:2317-23; PMID:2242760; http://dx.doi.org/10.1002/eji.1830201022.
43. Egan TJ. Recent advances in understanding the mechanism of hemozoin (malaria pigment) formation. J Inorg Biochem 2008; 102:1288-99; PMID:18226838; http://dx.doi.org/10.1016/j.jinorgbio.2007.12.004.
44. Jaramillo M, Godbout M, Olivier M. Hemozoin induces macrophage chemokine expression through oxidative stress-dependent and -independent mechanisms. J Immunol 2005; 174:475-84; PMID:15611273.

Journal of Virology

Full Conversion of the Hemagglutinin-Neuraminidase Specificity of the Parainfluenza Virus 5 Fusion Protein by Replacement of 21 Amino Acids in Its Head Region with Those of the Simian Virus 41 Fusion Protein

Masato Tsurudome, Mito Nakahashi, Yoshiaki Matsushima, Morihiro Ito, Machiko Nishio, Mitsuo Kawano, Hiroshi Komada and Tetsuya Nosaka

***J. Virol.* 2013, 87(15):8342. DOI: 10.1128/JVI.03549-12.**
Published Ahead of Print 22 May 2013.

JVI
Journals.ASM.org

Full Conversion of the Hemagglutinin-Neuraminidase Specificity of the Parainfluenza Virus 5 Fusion Protein by Replacement of 21 Amino Acids in Its Head Region with Those of the Simian Virus 41 Fusion Protein

Masato Tsurudome,[a] Mito Nakahashi,[a] Yoshiaki Matsushima,[a] Morihiro Ito,[b] Machiko Nishio,[d] Mitsuo Kawano,[a] Hiroshi Komada,[c] Tetsuya Nosaka[a]

Department of Microbiology and Molecular Genetics, Mie University Graduate School of Medicine, Tsu, Mie, Japan[a]; Department of Biomedical Sciences, College of Life and Health Sciences, Chubu University, Kasugai, Aichi, Japan[b]; Department of Microbiology, Suzuka University of Medical Science and Technology, Suzuka, Mie, Japan[c]; Department of Microbiology, Wakayama Medical University, Wakayama, Japan[d]

For most parainfluenza viruses, a virus type-specific interaction between the hemagglutinin-neuraminidase (HN) and fusion (F) proteins is a prerequisite for mediating virus-cell fusion and cell-cell fusion. The molecular basis of this functional interaction is still obscure partly because it is unknown which region of the F protein is responsible for the physical interaction with the HN protein. Our previous cell-cell fusion assay using the chimeric F proteins of parainfluenza virus 5 (PIV5) and simian virus 41 (SV41) indicated that replacement of two domains in the head region of the PIV5 F protein with the SV41 F counterparts bestowed on the PIV5 F protein the ability to induce cell-cell fusion on coexpression with the SV41 HN protein while retaining its ability to induce fusion with the PIV5 HN protein. In the study presented here, we furthered the chimeric analysis of the F proteins of PIV5 and SV41, finding that the PIV5 F protein could be converted to an SV41 HN-specific chimeric F protein by replacing five domains in the head region with the SV41 F counterparts. The five SV41 F-protein-derived domains of this chimera were then divided into 16 segments; 9 out of 16 proved to be not involved in determining its specificity for the SV41 HN protein. Finally, mutational analyses of a chimeric F protein, which harbored seven SV41 F-protein-derived segments, revealed that replacement of at most 21 amino acids of the PIV5 F protein with the SV41 F-protein counterparts was enough to convert its HN protein specificity.

The parainfluenza viruses (PIVs), which belong to the genus *Rubulavirus*, *Avulavirus*, or *Respirovirus* in the family *Paramyxoviridae*, have two kinds of glycoprotein spikes on the envelope: hemagglutinin-neuraminidase (HN) protein tetramers and fusion (F) protein trimers (1). The attachment protein HN is responsible for binding to the sialoconjugate receptors on the cell surface and for enzymatic destruction of the receptors, while the F protein mediates membrane fusion, such as cell-cell fusion or virus-cell fusion. Cleavage of the F precursor (F_0) by cellular proteases into disulfide-linked subunits F_1 and F_2 is a prerequisite for its fusion activity, similar to the other class I viral fusion proteins (1).

Unlike most of the other class I fusion proteins, however, the F protein does not have an apparent receptor-binding function. Moreover, most F proteins require a fusion-promoting function of the attachment protein HN in a virus type-specific manner (2, 3). Although it is not well-known how the HN protein promotes the F-protein-mediated membrane fusion, it is believed that the fusion is induced through a series of conformational changes of the F protein that are initiated by its specific interaction with the homologous HN protein (4–6). The fusion-promoting function of the HN protein appears to depend on it being bound to its cellular receptors (7–10), and the HN protein seems to promote the F-protein-mediated fusion in manner that is dependent on the balance between its inherent F-triggering efficiency and receptor-attachment regulatory functions (binding and destruction), as suggested by Porotto et al. (11). Furthermore, the presumptive signal-transducing activity of the HN protein may be required for the induction of cell-cell fusion (12).

On the one hand, the stalk region of the HN protein, which is a tetrameric coiled coil bundle structure (13, 14), is inferred to contain the site that determines the F-protein specificity in promoting fusion (15–17), while the head region carries both the receptor-binding and -destroying activities (18, 19). The involvement of the HN stalk region of an avulavirus, Newcastle disease virus, in the physical interaction with the F protein has been certified by coimmunoprecipitation analysis (20, 21). On the other hand, our previous chimeric analyses of the F proteins of two closely related rubulaviruses, human parainfluenza virus 2 (HPIV2) and simian virus 41 (SV41), suggested that a 144-amino-acid region (designated the middle region) in the ectodomain of the HPIV2 F protein contains the site(s) that determines its specificity for the HPIV2 HN protein in the induction of cell-cell fusion (22). Recently, we found that replacement of two domains in the head region of the PIV5 F protein with the SV41 F counterparts bestowed on the PIV5 F protein the ability to induce cell-cell fusion on coexpression with the SV41 HN protein without significantly affecting its ability to induce fusion with the PIV5 HN protein (23). Similarly, mutations of four amino acids in the head region of the F protein of canine distemper virus (CDV) strain Onderstepoort impair the ability to induce cell-cell fusion with the co-

Received 4 January 2013 Accepted 11 May 2013
Published ahead of print 22 May 2013
Address correspondence to Masato Tsurudome, turudome@doc.medic.mie-u.ac.jp.

doi:10.1128/JVI.03549-12

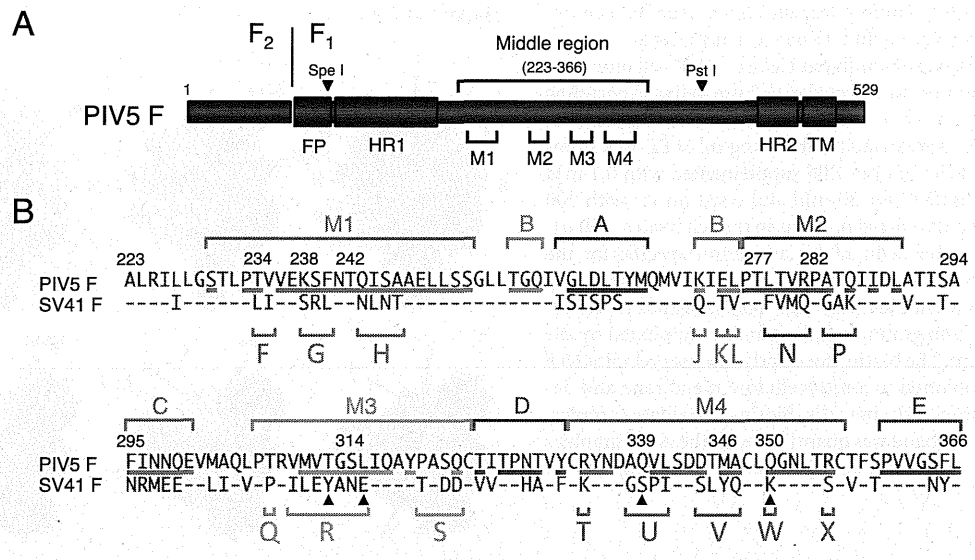

FIG 1 Division of five domains in the middle region of the PIV5 (WR) F protein into 16 segments. (A) Schematic diagram of the PIV5 F protein. The positions of four major domains (M1, M2, M3, and M4) in the middle region are indicated. The names of the restriction enzymes (SpeI and PstI), whose sites are present in the PIV5 F-encoding cDNA, indicate the corresponding positions in the PIV5 F polypeptides. The positions of heptad repeat regions 1 and 2 (HR1 and HR2) are based on the secondary structure of the HPIV3 F protein in its postfusion form (39). FP, fusion peptide; TM, transmembrane domain. (B) Amino acid sequence alignment of the middle regions of the F proteins of PIV5 and SV41. The positions of the four major domains and five minor domains (A, B, C, D, and E) are indicated above the amino acid sequences. Segments in each domain are indicated as capital letters below the amino acid sequences. Amino acid residues of the PIV5 F protein, which are exposed on the trimer surface, as described elsewhere (23), are underlined. Dashes in the SV41 F sequence indicate amino acids identical to those of the PIV5 F protein. The four filled triangles below the amino acid sequences of segments R, U, and W indicate the positions of the PIV5 F residues whose MV F counterparts are considered responsible for the H-F interaction (31).

expressed measles virus (MV) hemagglutinin (H) protein without significantly affecting the ability to induce fusion with the CDV H protein (24). CDV and MV are closely related members of the genus *Morbillivirus* in the family *Paramyxoviridae* (1).

It is noteworthy that replacement of the stalk region of a parainfluenza virus HN protein with that of another HN protein results in conversion of the F protein specificity (17, 23), being consistent with the involvement of the stalk region in the specific interaction with the homologous F protein. However, such a region of the F protein has not been identified. In the study presented here, we furthered the chimeric analysis of the F proteins of PIV5 and SV41 and found that replacement of 21 amino acids on the PIV5 F trimer surface with the SV41 F counterparts resulted in full conversion of HN protein specificity.

MATERIALS AND METHODS

Cells and recombinant plasmids. Monolayers of HeLa and BHK cells were maintained in Eagle's minimum essential medium (MEM) supplemented with 5% fetal calf serum (25, 26). The recombinant SRα plasmid encoding the HN or F protein of SV41 was described previously (17). The recombinant SRα plasmid encoding the HN protein of PIV5 strain W3A or that encoding the F protein of PIV5 strain WR was described elsewhere (27, 28). The WR F protein was used because it induced fusion only when coexpressed with the HN protein, whereas the W3A F protein was not used because it induced fusion even in the absence of the HN protein (27). The W3A HN protein was used instead of the WR HN protein because the former exhibited higher fusion-promoting activity than the latter when coexpressed with the PIV5 (WR) F protein (our unpublished data).

Generation of chimeric F proteins. To generate a chimeric F protein of SV41 and PIV5, a desired domain of the SV41 F-encoding plasmid was amplified by PCR, while both of the flanking regions of the corresponding domain of the PIV5 F-encoding plasmid were amplified while simultaneously introducing the restriction enzyme site for SpeI or PstI at the distal end, as described recently (23). These three fragments were then combined stepwise by fusion PCR and inserted into the PIV5 F-protein-encoding plasmid by utilizing restriction enzyme sites SpeI and PstI in the PIV5 F-encoding cDNA (Fig. 1A).

Quantification of cell-cell fusion. Subconfluent HeLa or BHK cell monolayers in six-well culture plates were transfected with 2 μg/well of F-encoding plasmid and 1 μg/well of HN-encoding plasmid by using Lipofectamine LTX reagent (Invitrogen) and an X-tremeGENE 9 DNA transfection kit (Roche), respectively. After 24 h (HeLa cells) or 12 h (BHK cells) of incubation at 37°C, the cells were fixed with 4% paraformaldehyde in phosphate-buffered saline (PBS), washed three times with PBS, and stained with Giemsa's solution. A photomicrograph which involved approximately 2.5×10^4 cells was taken, and the areas (number of pixels) occupied by the fused cells (or syncytia) were measured with the aid of graphics software, NIH ImageJ, version 1.45s. Then, the extent of cell fusion was estimated as the percentage of the syncytial areas to the total area of the photograph. Ten randomly taken photographs were measured for each sample, and the average fusion index (in percent) and standard deviation were determined.

Western blotting. Subconfluent HeLa or BHK cell monolayers were transfected with 2 μg/well of F-encoding plasmid as described above. After 24 h (HeLa cells) or 12 h (BHK cells) of incubation at 37°C, the cells were lysed on ice with 500 μl/well of lysis buffer (50 mM HEPES [pH 7.3], 10 mM lauryl maltoside, 1 mM phenylmethylsulfonyl fluoride, 100 mM NaCl), as reported previously (29). An aliquot (15 μl) of each cell lysate was subjected to sodium dodecyl sulfate-polyacrylamide gel electrophoresis (SDS-PAGE) under reducing conditions, and the separated proteins were electroblotted to a nitrocellulose membrane (Whatman). The membrane was then successively treated with monoclonal antibody 1D1 specific for a region (residues 448 to 452) immediately upstream of the heptad repeat 2 region of the PIV5 F_1 subunit (29), biotinylated horse immunoglobulin specific for mouse IgG (Vector Laboratories), and streptavidin-biotin-peroxidase complex (Vector Laboratories). The F-protein bands were then visualized by enhanced chemiluminescence

(ECL) using a Western blotting luminol reagent (Santa Cruz Biotechnology), followed by exposure to X-ray film (Konica, Tokyo, Japan).

Cell surface biotinylation. Subconfluent HeLa or BHK cell monolayers in six-well culture plates were transfected with 2 μg/well of F-encoding plasmid as described above. After 24 h (HeLa cells) or 12 h (BHK cells) of incubation at 37°C, the cells were treated with 0.3 mg/ml of EZ-link sulfo-NHS-LC-biotin (Thermo Scientific) in PBS supplemented with 0.1 mM $CaCl_2$ and 1 mM $MgCl_2$ at 23°C for 30 min and lysed on ice with 500 μl/well of lysis buffer. The biotinylated proteins in the cell lysates (150 μl) were then immunoprecipitated with rabbit antiserum specific for the PIV5 F_2 subunit (28) and subjected to SDS-PAGE under nonreducing conditions, because we could not identify the F-protein bands under reducing conditions due to comigrating cellular bands precipitated by the anti-F_2 peptide rabbit serum. The biotinylated and immunoprecipitated F proteins were then electroblotted to a nitrocellulose membrane and detected by ECL after treating with streptavidin-biotin-peroxidase complex. The intensity of the F-protein band was quantified with the aid of graphics software, NIH ImageJ, version 1.45s, and the relative surface expression level was estimated.

RESULTS

Replacement of five domains in the middle region of the PIV5 F protein with those of the SV41 F protein converts its HN protein specificity. Previously, we performed chimeric analysis of the F proteins of PIV5 and SV41 in order to determine the site(s) that determines the HN protein specificity of the F protein. In brief, the middle region of the PIV5 F protein was divided into four trimer surface-exposed major domains and five minor domains (23) (Fig. 1A and B). These nine domains were then replaced with the SV41 F counterparts individually or in various combinations, and the resultant chimeric F proteins were expressed in HeLa cells together with the HN protein of PIV5 or SV41. The results indicated that replacement of the domains M1 and M2, which harbored 16 noncontiguous amino acids that were not conserved between the F proteins, enabled the PIV5 F protein to functionally interact with the SV41 HN protein, inducing cell-cell fusion in HeLa cells (23). In addition to the two domains identified, M1 and M2, the SV41 F-derived domains M4 and B seemed to be involved in the functional interaction with the SV41 HN protein (23). However, any chimeric PIV5 F proteins that could induce fusion with the SV41 HN protein also induced fusion with the PIV5 HN protein (23). We thus intended to create a chimeric PIV5 F protein which would show clear specificity for the SV41 HN protein by replacing its four domains (M1, M2, M4, and B), which had been regarded to be important for determining the HN protein specificity, as described above, with the corresponding domains of the SV41 F protein. To our disappointment, the resultant chimera, B + M(1 + 2 + 4) did not induce cell-cell fusion in HeLa cells either with the SV41 HN protein or with the PIV5 HN protein (see Fig. 3D), presumably because the cleaved form (F_{1+2}) of this chimera was poorly expressed on the cell surface (see Fig. 3B). After our several attempts, however, it turned out that replacement of the domain M3, in addition to the four domains mentioned above, resulted in the chimera B + M(1 + 2 + 3 + 4), which was able to induce weak fusion (approximate fusion index, 1%) only when coexpressed with the SV41 HN protein (see Fig. 3D), though its cleaved form was weakly expressed on the cell surface, like that of B + M(1 + 2 + 4) was (see Fig. 3B and Fig. 5A). Interestingly, however, when we employed BHK cells for the cell-cell fusion assay, B + M(1 + 2 + 3 + 4) induced remarkable fusion (fusion index, 20.6% ± 1.9%) only when coexpressed with the SV41 HN protein (see Fig. 3E and Fig. 5B). In view of the findings that the extent of fusion induced by coexpression of the SV41 HN and F proteins in BHK cells was 19.6% ± 0.8% (data not shown), while that induced by coexpression of the PIV5 HN and F proteins was 12.6% ± 1.4% (see Fig. 5B), we have concluded that B + M(1 + 2 + 3 + 4) is an SV41 HN-specific protein similar to the SV41 F protein. This chimera harbored 41 SV41 F-derived amino acids, 32 of which were regarded as being exposed on the F trimer surface (Fig. 1B and Fig. 2). It was noteworthy, on the one hand, that the above-mentioned B + M(1 + 2 + 4) could not also induce fusion in BHK cells, whereas its cleaved form was expressed on the cell surface more abundantly than that of B + M(1 + 2 + 3 + 4) was (Fig. 3C and E).

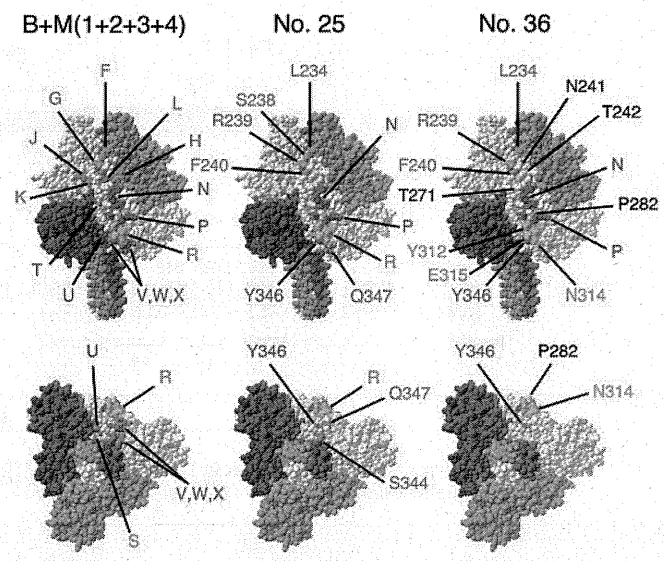

FIG 2 Positions of SV41 F-derived segments or amino acids in chimeric PIV5 F proteins. (Top) Side views of the F trimers; (bottom) bottom views of the F trimers. The SV41 F-derived segments and amino acids, which are exposed on the trimer surface, are indicated in the colors representing the domains they belong to (Fig. 1B); for simplicity, those in only one monomer are shown. The amino acids shown in black indicate those that intervene among the SV41 F-derived amino acids in chimera no. 36. The figure was prepared with the aid of the Deep View Swiss-Pdb Viewer program on the basis of the crystal structure of the PIV5 (W3A) F-cleavage-site mutant FR3 (Protein Data Bank accession number 2B9B) (40).

These results have indicated that the PIV5 F protein can be converted to an SV41 HN-specific chimeric F protein by replacement of its five domains (M1, M2, M3, M4, and B) with those of the SV41 F protein.

On the other hand, B + M2 and B + M(1 + 2) showed clear specificity for the PIV5 HN protein in HeLa cells (Fig. 3D). Interestingly, they induced prominent fusion in BHK cells irrespective of the presence of the HN protein (Fig. 3E). Nonetheless, their specificity for the PIV5 HN protein also seemed to be apparent in BHK cells, because their fusion indices with the PIV5 HN protein were significantly higher than those with the SV41 HN protein, which were similar to the fusion indices without the HN protein (Fig. 3E). Consistent with this observation, we have recently reported that the HN-independent fusion activity of the chimera B + M(1 + 2) was further promoted by the SV41 HN protein but not by the Newcastle disease virus HN protein (23). Accordingly, when a certain chimeric F protein exhibited HN-independent fusion activity, we regarded the fusion index to be the background and its HN protein specificity could be estimated only when it

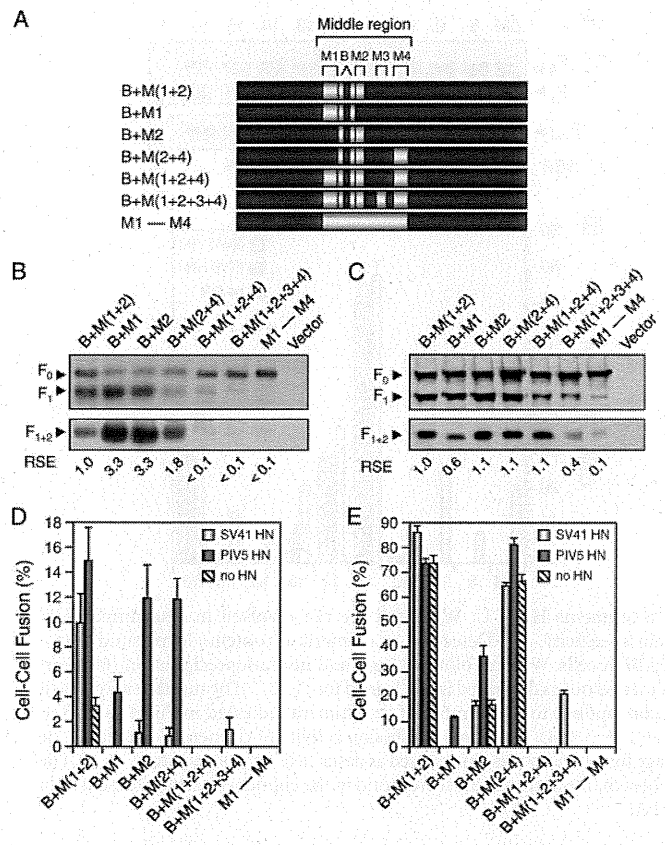

FIG 3 Replacement of five domains in the middle region of the PIV5 F protein with those of the SV41 F protein converts HN protein specificity. (A) Schematic diagram of chimeric F proteins. Dark boxes represent amino acid regions derived from the PIV5 F protein, while bright boxes represent the domains derived from the SV41 F protein. (B and C) Detection of chimeric F proteins in plasmid-transfected cells. Subconfluent HeLa (B) or BHK (C) cell monolayers in six-well culture plates were transfected with the recombinant plasmid encoding each F protein and lysed at 24 h (B) or 12 h (C) posttransfection. To detect the F proteins in the plasmid-transfected cells, the total cell lysates were subjected to SDS-PAGE under reducing conditions, followed by Western blotting with an anti-F_1 monoclonal antibody (top). To detect the F proteins expressed on the cell surface, the plasmid-transfected cells were biotinylated, the cell lysates were subjected to immunoprecipitation with anti-F_2 rabbit serum, and the precipitates were analyzed by SDS-PAGE under nonreducing conditions; the biotinylated F-protein band detected by immunoprecipitation represents the cleaved from (F_{1+2}), as reported previously (29) (bottom). The relative surface expression (RSE) level of the F proteins is presented below each lane. (D and E) Fusion activity of the chimeric F proteins. For analyzing the HN protein specificity of the F proteins in a cell-cell fusion assay, subconfluent HeLa (D) or BHK (E) cell monolayers in six-well culture plates were transfected with 2 μg/well of the recombinant SRα plasmid encoding each F protein together with 1 μg/well of the recombinant SRα plasmid encoding the SV41 HN protein or the PIV5 HN protein or with the SRα plasmid (no HN). After 24 h (D) or 12 h (E), the cells were fixed with 4% paraformaldehyde and the average fusion index was determined as described in Materials and Methods; error bars indicate standard deviations.

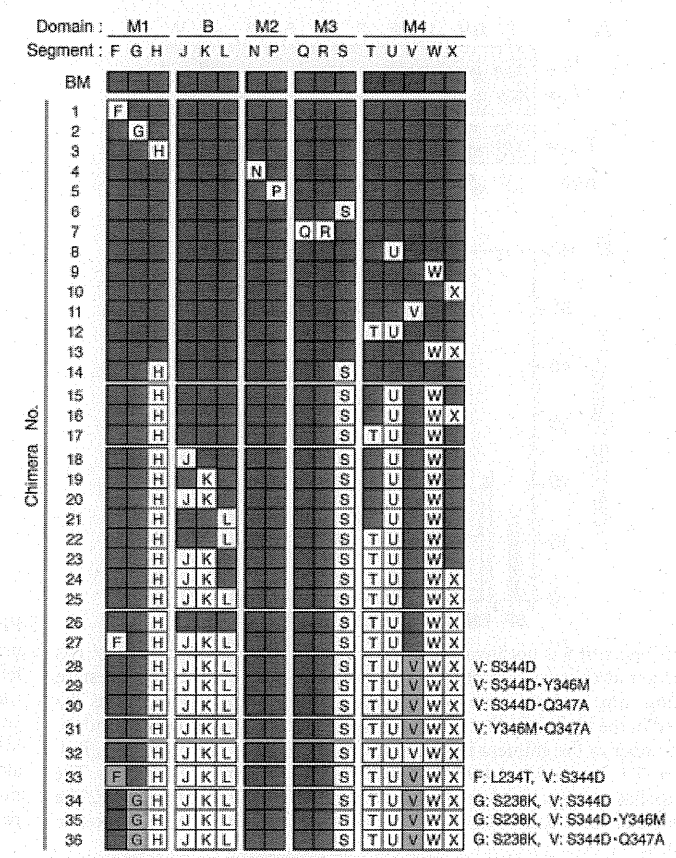

FIG 4 Structures of chimeric PIV5 F proteins. The chimeric structure of each chimera is shown as a set of 16 squares which correspond to the 16 segments shown in Fig. 1B. Dark gray squares, SV41 F-derived segment; white squares, PIV5 F-derived segment; light gray squares, SV41 F-derived segment F, G, or V with a mutation(s), details of which are shown on the right side of each chimera. The name of each segment is indicated only in the white and gray squares. BM, B + M(1 + 2 + 3 + 4).

induced fusion with either of the HN proteins at a level significantly higher than the background.

Segment S is not involved in determining HN protein specificity. In order to identify the SV41 F-derived amino acids that would be responsible for converting the PIV5 F protein to an SV41 HN-specific protein, the 41 amino acids in the five domains (M1, M2, M3, M4, and B), which were not shared by the F proteins of PIV5 and SV41, as described above, were grouped into 16 segments (Fig. 1B). Then, the SV41 F-derived segments of B + M(1 + 2 + 3 + 4) were then replaced with the PIV5 F counterparts individually or in combination, and the HN protein specificity of the resulting chimeric F proteins was investigated by using BHK cells; their chimeric structures are shown as schematics in Fig. 4.

To begin with, we focused on the eight segments in the domains M1, M2, and M3. As shown in Fig. 5B, SV41 F-derived segment S of B + M(1 + 2 + 3 + 4) could be replaced with the PIV5 F counterpart without affecting the prominent specificity for the SV41 HN protein, as represented by chimera no. 6, indicating that segment S is not involved in determining HN protein specificity. In contrast, chimera no. 2 exhibited low but apparent fusion activity (approximately 12%) with either of the HN proteins, indicating that SV41 F-derived segment G plays a critical role in determining HN protein specificity. Although chimera no. 1 induced moderate fusion even in the absence of the HN proteins, it induced fusion with the SV41 HN protein but not with the PIV5 HN protein at a level significantly higher than this background. This result suggested that segment F was not involved in determining HN protein specificity; we verified this assumption later on. On the other hand, chimeras no. 3, no. 4, and no. 5, whose cleaved forms were weakly expressed on the cell surface, did not show fusion activity with either of the HN proteins; thus, the role

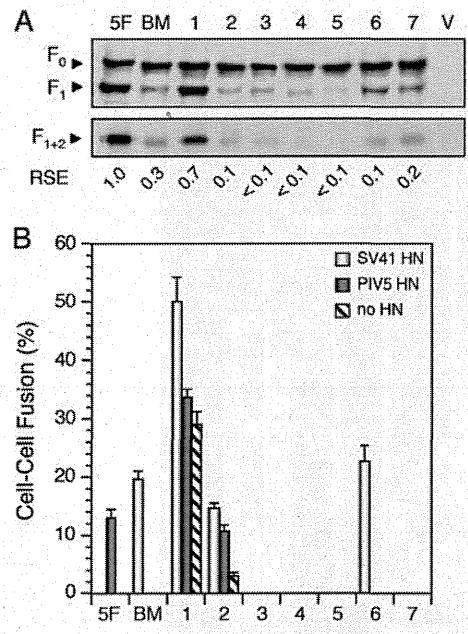

FIG 5 Segment S is not involved in determining HN protein specificity. (A) Detection of chimeric F proteins in plasmid-transfected BHK cells. Western blotting (top) and immunoprecipitation (bottom) were carried out as described in the legend for Fig. 3C. The number above each lane corresponds to the number of the chimera indicated in Fig. 4. 5F, PIV5 F protein; BM, B + M(1 + 2 + 3 + 4); V, vector. (B) Fusion activity of chimeric F proteins. The average fusion index was determined as described in the legend for Fig. 3E. The numbers on the abscissa axis correspond to the chimera numbers presented in panel A.

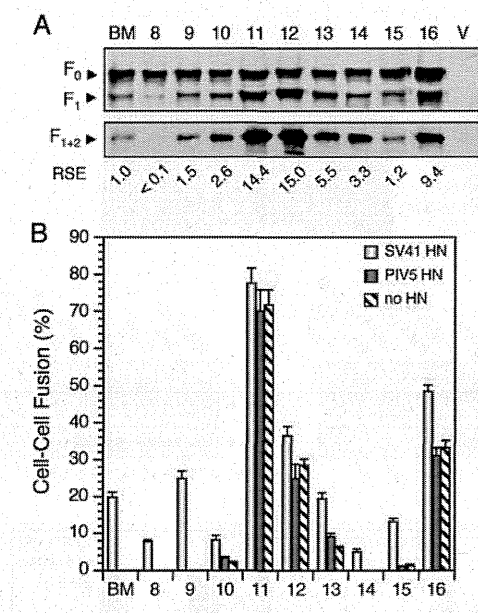

FIG 6 Segments H, T, U, W, and X are not involved in determining HN protein specificity. (A) Detection of chimeric F proteins in plasmid-transfected BHK cells. Western blotting (top) and immunoprecipitation (bottom) were carried out as described in the legend for Fig. 3C. The number above each lane corresponds to the number of the chimera indicated in Fig. 4. BM, B + M(1 + 2 + 3 + 4); V, vector. (B) Fusion activity of chimeric F proteins. The average fusion index was determined as described in the legend for Fig. 3E. The numbers on the abscissa axis correspond to the chimera numbers presented in panel A.

of segments H, N, and P could not be evaluated. The role of segments Q and R in determining HN protein specificity also remained unclear, since the corresponding chimera, no. 7, did not induce fusion with either of the HN proteins, even though the amount of its cleaved form on the cell surface was larger than that of chimera no. 6.

Segments H, T, U, W, and X are not involved in determining HN protein specificity. We then focused on the five segments in the domain M4 and found that SV41 F-derived segments U and W of B + M(1 + 2 + 3 + 4) could be replaced with the PIV5 HN counterparts without affecting the specificity for the SV41 HN protein, as represented by chimeras no. 8 and no. 9, respectively (Fig. 6B). Furthermore, replacement of segment X did not seem to affect the HN protein specificity of chimeras B + M(1 + 2 + 3 + 4) and no. 9, because the resultant chimeras, no. 10 and no. 13, respectively, induced fusion with the SV41 HN protein at levels significantly higher than their backgrounds but not with the PIV5 HN protein. These results suggested that segments U, W, and X are not involved in determining HN protein specificity. In contrast, replacement of segment V of B + M(1 + 2 + 3 + 4) resulted in chimera no. 11, which exhibited very high fusion activity (approximately 75%) independently of the coexpression with the HN protein, and thus, the role of V in determining HN protein specificity remained to be evaluated; we address this issue later on. Interestingly, replacement of segment T of chimera no. 8 resulted in chimera no. 12, which induced moderate HN-independent fusion (Fig. 6B). However, chimera no. 12 induced fusion with the SV41 HN protein at a level significantly higher than this background but not with the PIV5 HN protein. This result suggests that segment T is not involved in determining HN protein specificity.

As we described above, chimeras no. 6, no. 8, and no. 9 induced fusion only when coexpressed with the SV41 HN protein. Importantly, chimeras no. 6 and no. 9 induced fusion specifically with the SV41 HN protein even more prominently than the parent B + M(1 + 2 + 3 + 4) did. We then reassessed the role of segment H in domain M1 in the context of chimera no. 6, revealing that replacement of segment H with the PIV5 F counterpart reduced the fusion activity but did not affect the specificity for the SV41 HN protein, as represented by chimera no. 14 (Fig. 6B). This result thus suggested that segment H is not is not involved in determining HN protein specificity.

Taken together, the findings obtained so far have suggested that six segments (H, S, T, U, W, and X) are not involved in determining HN protein specificity. We then replaced these six segments of B + M(1 + 2 + 3 + 4) with those of the PIV5 F protein. As expected, the resultant chimera, no. 26, exhibited apparent specificity for the SV41 HN protein but it also showed moderate HN-independent fusion activity (Fig. 7B). Similarly, replacement of five segments (H, S, U, W, and X) of the six resulted in SV41 HN-specific chimera no. 16, which also showed HN-independent fusion activity (Fig. 6B). Intriguingly, when four segments (H, S, U, and W) of the six were replaced, the resultant chimera, no. 15, showed minimal HN-independent fusion and induced fusion specifically with the SV41 HN protein (Fig. 6B). Finally, replacement of segment T of chimera no. 15 resulted in chimera no. 17, which induced fusion specifically with the SV41 HN protein at a reduced level but showed no HN-independent fusion activity (Fig. 7B). These results were consistent with the

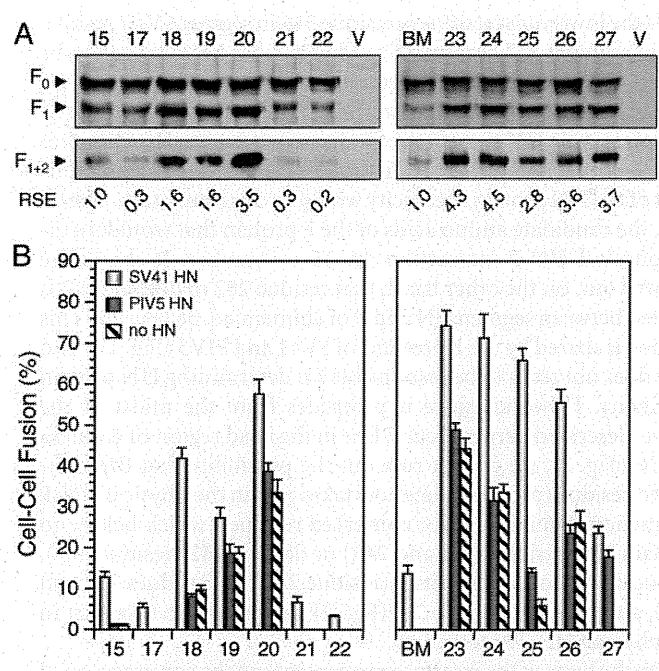

FIG 7 Domain B is not involved in determining HN protein specificity. (A) Detection of chimeric F proteins in plasmid-transfected BHK cells. Western blotting (top) and immunoprecipitation (bottom) were carried out as described in the legend for Fig. 3C. The number above each lane corresponds to the number of the chimera indicated in Fig. 4. BM, B + M(1 + 2 + 3 + 4); V, vector. (B) Fusion activity of chimeric F proteins. The average fusion index was determined as described in the legend for Fig. 3E. The numbers on the abscissa axis correspond to the chimera numbers presented in panel A.

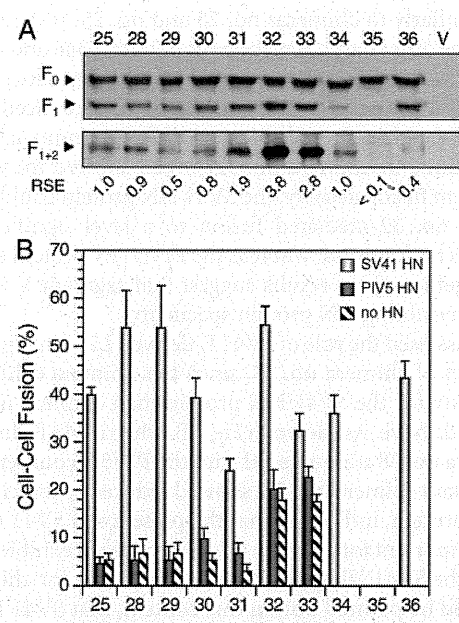

FIG 8 Segment V and residue 238 in segment G are not involved in determining HN protein specificity. (A) Detection of chimeric F proteins in plasmid-transfected BHK cells. Western blotting (top) and immunoprecipitation (bottom) were carried out as described in the legend for Fig. 3C. The number above each lane corresponds to the number of the chimera indicated in Fig. 4. V, vector. (B) Fusion activity of chimeric F proteins. The average fusion index was determined as described in the legend for Fig. 3E. The numbers on the abscissa axis correspond to the chimera numbers presented in panel A.

six segments not being involved in determining HN protein specificity.

Domain B is not involved in determining HN protein specificity. We then investigated the three segments J, K, and L in domain B in the context of SV41 HN-specific chimera no. 15, which showed negligible HN-independent fusion activity, as described above. As shown in Fig. 7B, segment J and/or segment K of chimera no. 15 could be replaced with the PIV5 F counterparts without affecting HN protein specificity, as represented by chimeras no. 18, no. 19, and no. 20, which induced fusion with the SV41 HN protein at levels significantly higher than their backgrounds but not with the PIV5 HN protein. In contrast, replacement of segment L of chimera no. 15 resulted in chimera no. 21, which induced fusion specifically with the SV41 HN protein but at a reduced level (Fig. 7B). Similar to chimera no. 15, replacement of segments J and K of chimera no. 17 resulted in chimera no. 23, which showed high HN-independent fusion activity but retained specificity for the SV41 HN protein, while replacement of segment L of chimera no. 17 resulted in chimera no. 22, which induced fusion specifically with the SV41 HN protein but at a reduced level (Fig. 7B). These results have suggested, unexpectedly, that the three segments in domain B are not involved in determining HN protein specificity.

Interestingly, we found after several attempts that replacement of segment X of chimera no. 23 reduced the HN-independent fusion activity without significantly affecting its fusion activity with the SV41 HN protein, as represented by chimera no. 24 (Fig. 7B). More interestingly, replacement of segment L of chimera no. 24 resulted in chimera no. 25, which induced fusion specifically with the SV41 HN protein to a similar extent but showed remarkably reduced HN-independent fusion activity (Fig. 7B and Fig. 8B). Notably, when domain B of chimera no. 25 was replaced with the SV41 F counterpart, the resultant chimera, no. 26, showed decreased fusion activity with the SV41 HN protein and increased HN-independent fusion activity (Fig. 7B).

Segment V and residue 238 in segment G are not involved in determining HN protein specificity. As described above, chimera no. 25 exhibited prominent specificity for the SV41 HN protein. This chimera contained 19 trimer surface-exposed amino acids derived from the SV41 F protein, as calculated from Fig. 1B; the uppermost amino acid among the 19 was residue 234 in segment F (Fig. 2). We then intended to see whether replacement of SV41 F-derived segment F, in which only L234 is exposed on the trimer surface (Fig. 1B), with the PIV5 F counterpart, T234, would affect HN protein specificity. As shown in Fig. 7B, the resultant chimera, no. 27, induced moderate fusion either with the SV41 HN protein or with the PIV5 HN protein, indicating that the presence of SV41 F-derived segment F (most likely, L234) is critical for chimera no. 25 to exhibit clear specificity for the SV41 HN protein, whereas it is not critical in the context of B + M(1 + 2 + 3 + 4), as represented by chimera no. 1 (Fig. 5B). On the other hand, the lowermost amino acid among the 19 was residue S344 in segment V of chimera no. 25 (Fig. 2). Interestingly, replacement of SV41 F-derived S344 of chimera no. 25 with the PIV5 F counterpart, D344, resulted in chimera no. 28, which induced fusion with the SV41 HN protein more prominently than chimera no. 25 did (Fig. 8B). Furthermore, replacement of SV41 F-derived Y346 or Q347 in segment V of chimera no. 28 resulted in chimeras no. 29 and no. 30, respectively, which induced fusion specifically with the SV41

HN protein similarly to chimeras no. 28 and no. 25, respectively (Fig. 8B). On the other hand, replacement of both Y346 and Q347 of chimera no. 25 resulted in chimera no. 31, which induced fusion specifically with the SV41 HN protein but at a reduced level (Fig. 8B). Finally, although replacement of all the amino acids in segment V resulted in chimera no. 32, which showed increased HN-independent fusion activity, the SV41 HN protein could promote chimera no. 32-mediated fusion to a level significantly higher than this background, whereas the PIV5 HN protein could not. Taken together, these results suggest that segment V is not involved in determining HN protein specificity.

We then reassessed the role of SV41 F-derived L234 in segment F in the context of chimera no. 28, since this chimera exhibited clearer specificity for the SV41 HN protein than chimera no. 25 did, as described above. As shown in Fig. 8B, when SV41 F-derived L234 of chimera no. 28 was replaced with the PIV5 F counterpart, T234, the resultant chimera, no. 33, showed reduced specificity for the SV41 HN protein, indicating that the presence of SV41 F-derived L234 is important for chimera no. 28 in order to exhibit clear specificity for the SV41 HN protein, the same as it is for chimera no. 25. It should be pointed out, in this context, that SV41 F-derived L234 is in contact with SV41 F-derived S238 in segment G, as shown in Fig. 2 (no. 25, top). We therefore replaced SV41 F-derived S238 of chimera no. 28 with the PIV5 F counterpart, K238. Notably, the resultant chimera, no. 34, did not show HN-independent fusion activity, whereas it retained clear specificity for the SV41 HN protein (Fig. 8B).

Finally, we reassessed the roles of SV41 F-derived Y346 and Q347 in segment V in the context of chimera no. 34. Unfortunately, replacement of SV41 F-derived Y346 with the PIV5 F counterpart, M346, resulted in a fusion-deficient chimera, no. 35 (Fig. 8B), whose cleaved form was weakly expressed on the cell surface (Fig. 8A). Most notably, however, SV41 F-derived Q347 of chimera no. 34 could be replaced with the PIV5 F counterpart, A347, without affecting its clear specificity for the SV41 HN protein, as represented by chimera no. 36 (Fig. 8B). As shown in Fig. 1B and Fig. 2, chimera no. 36 harbored 21 SV41 F-derived amino acids, of which 16 were exposed on the trimer surface.

Taken together, the SV41 F-derived 21 amino acids of B + M(1 + 2 + 3 + 4), a chimeric PIV5 F protein that harbored 41 SV41 F-derived amino acids, could be replaced with the PIV5 F counterpart without affecting its clear specificity for the SV41 HN protein. In other words, replacement of the corresponding 21 amino acids of the PIV5 F protein with those of the SV41 F protein resulted in an F protein that exhibited clear specificity for the SV41 HN protein.

DISCUSSION

In the present study, we have shown that replacement of 21 amino acids of the PIV5 F protein with the SV41 F counterparts is enough to convert the PIV5 F protein to a protein specific for the SV41 HN protein, as represented by chimera no. 36. Importantly, 16 out of the 21 amino acids are exposed on the trimer surface (Fig. 1B and 2) and thus could be regarded as the candidates that directly mediate the physical interaction of the F protein with the HN protein. Interestingly, these 16 amino acids form into a noncontiguous and nearly perpendicular line on the lateral side of the head region of chimera no. 36 (Fig. 2), which is approximately 6 nm in length, as deduced from the total length (12 nm) of the PIV5 F trimer (30). The uppermost residue of this line is residue 234 in segment F, while the lowermost residue is residue 346 in segment V or residue 314 in segment R. Uppermost residue 234 has been proved to be critical for determining HN protein specificity, as represented by chimera no. 33. In contrast, lowermost residue 346 is not involved in determining HN protein specificity, as represented by chimeras no. 29, no. 31, and no. 32; evaluation of this residue as a determinant of the HN protein specificity would be our future task. Therefore, the candidate amino acids of the F protein that would mediate physical HN-F interaction are 15 in number. It should be pointed out, on the other hand, that residue 282 in domain M2 is located between segments N and P of chimera no. 36 (Fig. 2). This residue is shared by the F proteins of SV41 and PIV5 (Fig. 1B) and thus does not seem to be responsible for determining HN protein specificity. However, since it protrudes from the midst of the above-described perpendicular line in the head region of chimera no. 36 (Fig. 2), we cannot rule out the possibility that this conserved residue (proline) somehow takes part in the physical HN-F interaction. Similarly, three conserved residues, which belong to domain M1 (residues 241 and 242) or domain M2 (residue 277), are located among segments F (residue 234), G (residues 239 and 240), and N of chimera no. 36 (Fig. 2); they may also take part in the physical HN-F interaction.

On the basis of the interface propensity and the conservation of physical chemical properties among F proteins, it has been proved that six residues at the base of the MV F head region receive the signal from the MV H protein (31), suggesting that these residues are involved in the H-F interaction. It is worth noting, in this context, that two (Q322 and E325) of the identified six residues correspond to T312 and L315 in PIV5 F segment R, respectively (Fig. 1B and Fig. 2), which are the constituents of the 15 candidates that would mediate the HN-F interaction, as described above. However, another two (Y349 and R360) of the six residues correspond to Q339 in segment U and Q350 in segment W, respectively (Fig. 1B), which proved not to be important for the HN-F interaction. The remaining two (Q383 and L394) correspond to PIV5 F residues D373 and L384, respectively, which are not included in the middle region and thus may not be involved in the HN-F interaction. Notably, in this context, three CDV F residues that are considered to be involved in the H-F interaction are located in F_2 or in the fusion peptide (24). Taken together, these findings suggest that the sites of the rubulavirus F protein interacting with the HN protein are only partially identical to the sites of the morbillivirus F protein interacting with the H protein, which would reflect a difference in the mechanisms of F activation between the two genera (4).

Our previous chimeric analysis revealed that a chimeric PIV5 F protein which harbored four SV41 F-derived domains (M1, M2, M3, and M4), or, in other words, 38 SV41 F-derived amino acids (Fig. 1B), induced fusion either with the PIV5 HN protein or with the SV41 HN protein (23). We found in the present study, however, that replacement of only 21 amino acids in these four domains is enough to convert the PIV5 F protein to an SV41 HN-specific protein. Thus, whether a given chimeric PIV5 F protein interacts with the SV41 HN protein or with the PIV5 HN protein does not simply reflect the number of SV41 F-derived amino acids, suggesting that the tertiary and/or quaternary structure of the putative HN-interacting site of the chimeric PIV5 F protein seems to be extremely important for determining its HN protein specificity. In other words, the role of a given SV41 F-derived domain or amino acid in the interaction with the SV41 HN protein may

vary in a manner that is dependent on the structure of the respective chimeric PIV5 F protein, since it is very likely that the conformation and/or relative position of the SV41 F-derived domains or amino acids in the context of a chimeric F protein may differ from that in another chimeric F protein or from that in the SV41 F protein. Such a difference would be enough to discriminate between an SV41 HN-specific structure and a cross-reactive structure.

Although it is appreciated that the HN-F interaction is virus type specific, the HPIV2 HN protein is able to substitute for the HN proteins of SV41 and HPIV4A (17), while the HN protein of mumps virus can substitute for the HN proteins of HPIV2 and PIV5 (22, 27). Such cross-reactivity of some HN proteins cannot simply be explained by their proximity to the substitutable HN proteins in terms of primary structure, since the converse heterotypic combinations of the HN and F proteins result in no fusion (17, 22). We thus speculate that similarity in the tertiary and/or quaternary structure between the stalk regions of the HN proteins is also crucial for their compatibility; a subtle difference might result in the one-way cross-reactivity, as we have suggested elsewhere (32). It is important to point out, in this context, that a given HN (or F) protein has the potential to substitute for another HN (or F) protein when the overall amino acid sequence identity between the proteins is 39% (or 36%) or greater (22, 32). It is thus important to note that the SV41 F protein cannot substitute for the PIV5 F protein and vice versa, despite the fact that their amino acid sequence identity is 49.9% (23, 33), which, fortunately, enabled us to perform the chimeric analyses of their F proteins.

A number of chimeric F proteins created in the present study displayed HN-independent fusion activity; above all, chimera no. 11 exhibited hyperfusogenic activity in the absence of the HN protein (Fig. 6B), indicating that SV41 F-derived segment V somehow contributes to this phenotype. Consistently, replacement of segment V of chimera no. 25 with the SV41 F counterpart resulted in chimera no. 32, which showed increased HN-independent fusion activity (Fig. 8B). Similarly, SV41 F-derived segments F, J, K, and X also seemed to contribute to HN-independent fusion activity in the context of some chimeras, for example, no. 1, no. 18, no. 19, and no. 16, respectively. With regard to this issue, it is known that introduction of several mutations into the PIV5 F protein bestows HN-independent fusion activity on the F protein (27, 34, 35). These mutations are considered to destabilize the F protein so that it can undergo the conformational changes that lead to fusion in the absence of the HN protein (36). Therefore, if the physical interaction between the HN stalk region and the putative HN-interacting region of the F protein results in destabilization of the F protein, then mutation or chimeric recombination of the HN-interacting region or its franking region might result in destabilization of the F protein in some cases, as we have recently postulated (23).

Intriguingly, the fusion activities of most chimeric F proteins in BHK cells at 12 h posttransfection are much higher than those in HeLa cells at 24 h posttransfection, as represented by the chimeras shown in Fig. 3D and E. Notably, B + M(1 + 2) and B + M(2 + 4) induced hyperfusogenic activity in BHK cells independently of the coexpressed HN protein. This finding indicates, importantly, that the difference in the fusion activity of a given chimera between the two cell lines cannot simply be explained by the possible difference in the surface expression level of the chimera and/or in the amount of cellular receptors for the HN protein. Rather, it seems likely that these cell lines differ in the lipid composition of the plasma membrane, in the integrity of the cytoskeleton, such as that of cortical actin, or in the amount of a putative receptor(s) for the F protein, any one of which would account for the different susceptibilities of the two cell lines to the intrinsic fusion activity of the F proteins. Importantly, in this context, it has been reported that cellular transmembrane molecules, such as interferon-inducible transmembrane protein 1 (IFITM1) or CD98 heavy chain, regulate the cell-cell fusion induced by viral glycoproteins (37, 38). Possible differences in the functions of these cellular fusion regulatory proteins between the two cell lines may account for the higher fusion activity of the chimeras in BHK cells. Intriguingly, on the other hand, the difference in the surface expression levels between the chimeras in BHK cells seems much less than that in HeLa cells (Fig. 3B and C), suggesting that there may be differences in the transport machinery and/or in the quality control mechanism between the two cell lines.

The cleaved form (F_{1+2}) of some chimeras, including B + M(1 + 2 + 3 + 4), is poorly expressed on the BHK cell surface compared to the expression of the PIV5 F protein, but this phenotype does not seem to correlate either with the chimeric structure, with the HN protein specificity, or with HN independence. Interestingly, on the one hand, the data from Western blotting of the total cell lysate indicate that the amounts of the cleaved form (F_1) of these chimeras are also considerably smaller than those of the chimeras whose F_{1+2} forms are efficiently expressed on the cell surface. In contrast, the amounts of the uncleaved form (F_0) of most chimeras are similar regardless of their surface expression efficiency. These findings thus indicate that the above-mentioned paucity in the amount of the cell surface-expressed F_{1+2} cannot simply be explained by low cleavage efficiency. Provided that there is no difference in translation efficiency, it is possible that those chimeras whose F_{1+2} forms are poorly expressed on the cell surface are degraded after cleavage. In all likelihood, their F_{1+2} forms may be structurally labile, which would result in their transport to the late endosome/lysosome for degradation either directly from the *trans*-Golgi network or from the cell surface. Although it is possible that these chimeras are prone to undergo misfolding in the endoplasmic reticulum and thus are retrotranslocated to the cytoplasm for degradation in the proteasome, such degradation would result in small amounts not only of the cleaved form but also of the uncleaved form.

ACKNOWLEDGMENT

This work was supported by a Grant-in-Aid for Scientific Research (grant 23590538) from the Ministry of Education, Culture, Sports, Science and Technology, Japan.

REFERENCES

1. **Lamb RA, Parks GD.** 2007. *Paramyxoviridae*: the viruses and their replication, p 1449–1496. *In* Knipe DM, Howley PM, Griffin DE, Lamb RA, Martin MA, Roizman B, Straus SE (ed), Fields virology, 5th ed, vol 1. Lippincott Williams & Wilkins, Philadelphia, PA.
2. **Heminway BR, Yu Y, Galinski MS.** 1994. Paramyxovirus mediated cell fusion requires co-expression of both the fusion and hemagglutinin-neuraminidase glycoproteins. Virus Res. 31:1–16.
3. **Hu X, Ray R, Compans RW.** 1992. Functional interactions between the fusion protein and hemagglutinin-neuraminidase of human parainfluenza viruses. J. Virol. 66:1528–1534.
4. **Iorio RM, Melanson VR, Mahon PJ.** 2009. Glycoprotein interactions in paramyxovirus fusion. Future Virol. 4:335–351.

5. **Lamb RA, Jardetzky TS.** 2007. Structural basis of viral invasion: lessons from paramyxovirus F. Curr. Opin. Struct. Biol. **17**:427–436.
6. **Morrison TG.** 2003. Structure and function of a paramyxovirus fusion protein. Biochim. Biophys. Acta **1614**:73–84.
7. **McGinnes LW, Morrison TG.** 2006. Inhibition of receptor binding stabilizes Newcastle disease virus HN and F protein-containing complexes. J. Virol. **80**:2894–2903.
8. **Moscona A, Peluso RW.** 1991. Fusion properties of cells persistently infected with human parainfluenza virus type 3: participation of hemagglutinin-neuraminidase in membrane fusion. J. Virol. **65**:2773–2777.
9. **Moscona A, Peluso RW.** 1992. Fusion properties of cells infected with human parainfluenza virus type 3: receptor requirements for viral spread and virus-mediated membrane fusion. J. Virol. **66**:6280–6287.
10. **Russell CJ, Jardetzky TS, Lamb RA.** 2001. Membrane fusion machines of paramyxoviruses: capture of intermediates of fusion. EMBO J. **20**:4024–4034.
11. **Porotto M, Murrell M, Greengard O, Doctor L, Moscona A.** 2005. Influence of the human parainfluenza virus 3 attachment protein's neuraminidase activity on its capacity to activate the fusion protein. J. Virol. **79**:2383–2392.
12. **Tsurudome M, Nishio M, Ito M, Tanahashi S, Kawano M, Komada H, Ito Y.** 2008. Effects of hemagglutinin-neuraminidase protein mutations on cell-cell fusion mediated by human parainfluenza type 2 virus. J. Virol. **82**:8283–8295.
13. **Bose S, Welch BD, Kors CA, Yuan P, Jardetzky T, Lamb RA.** 2011. Structure and mutagenesis of the parainfluenza virus 5 hemagglutinin-neuraminidase stalk domain reveals a four-helix bundle and the role of the stalk in fusion promotion. J. Virol. **85**:12855–12866.
14. **Yuan P, Swanson KA, Leser GP, Paterson RG, Lamb RA, Jardetzky TS.** 2011. Structure of the Newcastle disease virus hemagglutinin-neuraminidase (HN) ectodomain reveals a four-helix bundle stalk. Proc. Natl. Acad. Sci. U. S. A. **108**:14920–14925.
15. **Deng R, Mirza AM, Mahon PJ, Iorio RM.** 1997. Functional chimeric HN glycoproteins derived from Newcastle disease virus and human parainfluenza virus-3. Arch. Virol. **13**(Suppl):115–130.
16. **Tanabayashi K, Compans RW.** 1996. Functional interaction of paramyxovirus glycoproteins: identification of a domain in Sendai virus HN which promotes cell fusion. J. Virol. **70**:6112–6118.
17. **Tsurudome M, Kawano M, Yuasa T, Tabata N, Nishio M, Komada H, Ito Y.** 1995. Identification of regions on the hemagglutinin-neuraminidase protein of human parainfluenza virus type 2 important for promoting cell fusion. Virology **213**:190–203.
18. **Mirza AM, Sheehan JP, Hardy LW, Glickman RL, Iorio RM.** 1993. Structure and function of a membrane anchor-less form of the hemagglutinin neuraminidase glycoprotein of Newcastle disease virus. J. Biol. Chem. **268**:21425–21432.
19. **Thompson SD, Portner A.** 1987. Localization of functional sites on the hemagglutinin-neuraminidase glycoprotein of Sendai virus by sequence analysis of antigenic and temperature-sensitive mutants. Virology **160**: 1–8.
20. **Melanson VR, Iorio RM.** 2004. Amino acid substitutions in the F-specific domain in the stalk of the Newcastle disease virus HN protein modulate fusion and interfere with its interaction with the F protein. J. Virol. **78**: 13053–13061.
21. **Melanson VR, Iorio RM.** 2006. Addition of N-glycans in the stalk of the Newcastle disease virus HN protein blocks its interaction with the F protein and prevents fusion. J. Virol. **80**:623–633.
22. **Tsurudome M, Ito M, Nishio M, Kawano M, Okamoto K, Kusagawa S, Komada H, Ito Y.** 1998. Identification of regions on the fusion protein of human parainfluenza virus type 2 which are required for haemagglutinin-neuraminidase proteins to promote cell fusion. J. Gen. Virol. **79**:279–289.
23. **Tsurudome M, Ito M, Nishio M, Nakahashi M, Kawano M, Komada H, Nosaka T, Ito Y.** 2011. Identification of domains on the fusion (F) protein trimer that influence the hemagglutinin-neuraminidase specificity of the F protein in mediating cell-cell fusion. J. Virol. **85**:3253–3261.
24. **Lee JK, Prussia A, Paal T, White LK, Snyder JP, Plemper RK.** 2008. Functional interaction between paramyxovirus fusion and attachment proteins. J. Biol. Chem. **283**:16561–16572.
25. **Ito M, Nishio M, Kawano M, Komada H, Ito Y, Tsurudome M.** 2009. Effects of multiple amino acids of the parainfluenza virus 5 fusion protein on its haemagglutinin-neuraminidase-independent fusion activity. J. Gen. Virol. **90**:405–413.
26. **Tsurudome M, Ito M, Nishio M, Kawano M, Komada H, Ito Y.** 2001. Hemagglutinin-neuraminidase-independent fusion activity of simian virus 5 fusion (F) protein: difference in conformation between fusogenic and nonfusogenic F proteins on the cell surface. J. Virol. **75**:8999–9009.
27. **Ito M, Nishio M, Kawano M, Kusagawa S, Komada H, Ito Y, Tsurudome M.** 1997. Role of a single amino acid at the amino terminus of the simian virus 5 F2 subunit in syncytium formation. J. Virol. **71**:9855–9858.
28. **Ito M, Nishio M, Komada H, Ito Y, Tsurudome M.** 2000. An amino acid in the heptad repeat 1 domain is important for the haemagglutinin-neuraminidase-independent fusing activity of simian virus 5 fusion protein. J. Gen. Virol. **81**:719–727.
29. **Tsurudome M, Ito M, Nishio M, Kawano M, Komada H, Ito Y.** 2006. A mutant fusion (F) protein of simian virus 5 induces hemagglutinin-neuraminidase-independent syncytium formation despite the internalization of the F protein. Virology **347**:11–27.
30. **Connolly SA, Leser GP, Yin HS, Jardetzky TS, Lamb RA.** 2006. Refolding of a paramyxovirus F protein from prefusion to postfusion conformations observed by liposome binding and electron microscopy. Proc. Natl. Acad. Sci. U. S. A. **103**:17903–17908.
31. **Apte-Sengupta S, Negi S, Leonard VH, Oezguen N, Navaratnarajah CK, Braun W, Cattaneo R.** 2012. Base of the measles virus fusion trimer head receives the signal that triggers membrane fusion. J. Biol. Chem. **287**: 33026–33035.
32. **Tsurudome M.** 2011. Virus entry: parainfluenza viruses, p 35–61. *In* Ming L (ed), Negative strand RNA virus. World Scientific, Hackensack, NJ.
33. **Tsurudome M, Bando H, Kawano M, Matsumura H, Komada H, Nishio M, Ito Y.** 1991. Transcripts of simian virus 41 (SV41) matrix gene are exclusively dicistronic with the fusion gene which is also transcribed as a monocistron. Virology **184**:93–100.
34. **Russell CJ, Jardetzky TS, Lamb RA.** 2004. Conserved glycine residues in the fusion peptide of the paramyxovirus fusion protein regulate activation of the native state. J. Virol. **78**:13727–13742.
35. **Seth S, Vincent A, Compans RW.** 2003. Mutations in the cytoplasmic domain of a paramyxovirus fusion glycoprotein rescue syncytium formation and eliminate the hemagglutinin-neuraminidase protein requirement for membrane fusion. J. Virol. **77**:167–178.
36. **Paterson RG, Russell CJ, Lamb RA.** 2000. Fusion protein of the paramyxovirus SV5: destabilizing and stabilizing mutants of fusion activation. Virology **270**:17–30.
37. **Li K, Markosyan RM, Zheng YM, Golfetto O, Bungart B, Li M, Ding S, He Y, Liang C, Lee JC, Gratton E, Cohen FS, Liu SL.** 2013. IFITM proteins restrict viral membrane hemifusion. PLoS Pathog. **9**:e1003124. doi:10.1371/journal.ppat.1003124.
38. **Tsurudome M, Ito Y.** 2000. Function of fusion regulatory proteins (FRPs) in immune cells and virus-infected cells. Crit. Rev. Immunol. **20**: 167–196.
39. **Yin HS, Paterson RG, Wen X, Lamb RA, Jardetzky TS.** 2005. Structure of the uncleaved ectodomain of the paramyxovirus (hPIV3) fusion protein. Proc. Natl. Acad. Sci. U. S. A. **102**:9288–9293.
40. **Yin HS, Wen X, Paterson RG, Lamb RA, Jardetzky TS.** 2006. Structure of the parainfluenza virus 5 F protein in its metastable, prefusion conformation. Nature **439**:38–44.

HUMAN GENE THERAPY 24:683–691 (July 2013)

DOI: 10.1089/hum.2013.024

Human Parainfluenza Virus Type 2 Vector Induces Dendritic Cell Maturation Without Viral RNA Replication/Transcription

Kenichiro Hara,[1] Masayuki Fukumura,[1,2] Junpei Ohtsuka,[1,2] Mitsuo Kawano,[1] and Tetsuya Nosaka[1]

Abstract

The dendritic cell (DC), a most potent antigen-presenting cell, plays a key role in vaccine therapy against infectious diseases and malignant tumors. Although advantages of viral vectors for vaccine therapy have been reported, potential risks for adverse effects prevent them from being licensed for clinical use. Human parainfluenza virus type 2 (hPIV2), one of the members of the *Paramyxoviridae* family, is a nonsegmented and negative-stranded RNA virus. We have developed a reverse genetics system for the production of infectious hPIV2 lacking the *F* gene (hPIV2ΔF), wherein various advantages for vaccine therapy exist, such as cytoplasmic replication/transcription, nontransmissible infectivity, and extremely high transduction efficacy in various types of target cells. Here we demonstrate that hPIV2ΔF shows high transduction efficiency in human DCs, while not so high in mouse DCs. In addition, hPIV2ΔF sufficiently induces maturation of both human and murine DCs, and the maturation state of both human and murine DCs is almost equivalent to that induced by lipopolysaccharide. Moreover, alkylating agent β-propiolactone-inactivated hPIV2ΔF (BPL-hPIV2ΔF) elicits DC maturation without viral replication/transcription. These results suggest that hPIV2ΔF may be a useful tool for vaccine therapy as a novel type of paramyxoviral vector, which is single-round infectious vector and has potential adjuvant activity.

Introduction

VACCINE THERAPY has been expected to prevent pathogenic infections and malignant tumors. Until now, to acquire sufficient vaccine effects in the human body, many vaccine-delivering systems and adjuvants have been developed (Liu, 2010; Bolhassani *et al.*, 2011; Alving *et al.*, 2012; Goutagny *et al.*, 2012). Dendritic cells (DCs) are often targeted for vaccine delivery because the DC is a professional antigen-presenting cell (APC) and has a pivotal role in generating vaccine-specific immune responses. Therefore, *in vivo* DC-targeted vaccines or *ex vivo* DC therapies have been developed (Gilboa, 2007; Tacken and Figdor, 2011). On viral infection, DCs mature into effective APCs to activate naive T cells. By maturation, DCs express high levels of surface molecules (e.g., MHC-I, MHC-II, and costimulatory molecules) and secrete various cytokines (Lo *et al.*, 2006). Because the maturation state of DCs affects the balance between immunity and tolerance, or T cell polarizations (Guermonprez *et al.*, 2002; Feili-Hariri *et al.*, 2005; Kaiko *et al.*, 2008), efficient delivery of the vaccine antigen into DCs and simultaneous induction of DC maturation are important for generating T cell immunity.

Viral vectors are superior to other systems because of their high efficiency of transduction into DCs as a part of the natural infection process and because of their strong DC-stimulatory activity (Jenne *et al.*, 2001; Breckpot *et al.*, 2004). Although several clinical candidates have been reported, their unexpected adverse effects (e.g., severe inflammation and carcinogenesis) or poor immunogenicity has similarly been pointed out (Thomas *et al.*, 2003). Thus, to overcome these problems, it has been desired to develop novel types of viral vectors.

Human parainfluenza virus type 2 (hPIV2), a member of the genus *Rubulavirus* in the *Paramyxoviridae* family, is a respiratory pathogen responsible for acute respiratory tract illness, especially among children (Weinberg *et al.*, 2009), but not in adults. The hPIV2 genome is nonsegmented and negative-stranded RNA, which encodes seven proteins. The viral genes line up in the following order: 3′-(leader)-NP-P/V-M-F-HN-L-(trailer)-5′. The P and L proteins bind to nucleocapsid (RNA encompassed by nucleoprotein [NP]) to

[1]Department of Microbiology and Molecular Genetics, Mie University Graduate School of Medicine, Tsu, Mie 514-8507, Japan.
[2]Biocomo, Komono, Mie 510-1233, Japan.

form the ribonucleoprotein (RNP) complex. The hPIV2 envelope contains two glycoproteins, namely the HN and F proteins, and their cytoplasmic tails bind to the M protein, which lies on the viral envelope (Kawano *et al.*, 2001; Henrickson, 2003). Of the viral envelope proteins, the F protein has fusion activity and it reciprocally works with the HN protein to achieve viral envelope-to-cell or cell-to-cell fusion (Tsurudome *et al.*, 2008). Previous studies demonstrated that Sendai virus (mouse parainfluenza virus type 1) lacking the *F* gene (SeVΔF) can be self-replicative, but not infect neighboring cells. SeVΔF carrying an exogenous antigen gene efficiently transduces the antigen into DCs and induces antigen-specific immunity *in vivo* without any side effects (Li *et al.*, 2000; Ferrari *et al.*, 2004; Shibata *et al.*, 2006; Yoneyama *et al.*, 2007; Duan *et al.*, 2009). These data suggest that SeVΔF is safe and effective for vaccine therapy in comparison with conventional viral vectors.

Using reverse genetics technology, we have developed hPIV2 lacking the *F* gene (hPIV2ΔF) from the recombinant hPIV2 cDNA (Ohtsuka *et al.*, manuscript in preparation), and infectious hPIV2ΔF carrying the jellyfish gene encoding enhanced green fluorescent protein (*EGFP*) has been successfully recovered from a novel cell line stably expressing hPIV2 F protein. In addition, hPIV2ΔF infects a broad range of cells and shows nontransmissible infectivity, suggesting that hPIV2ΔF is a potentially promising novel paramyxovirus-based vector.

Here we demonstrate the fundamental immunogenic property of hPIV2ΔF, using human and murine DCs *in vitro*. hPIV2ΔF transduced an exogenous antigen into human DCs more efficiently compared with a conventional retroviral vector in transient assays. Although viral genomic copy numbers of hPIV2ΔF were significantly lower in murine DCs than in human DCs, similar maturation of both DC types was induced after infection. Moreover, DC maturation was found to be induced by preexisting hPIV2ΔF components without viral replication/transcription, implicating adjuvant activity by themselves.

Materials and Methods

Cell lines

The PLAT-gp packaging cell line, kindly provided by T. Kitamura (Division of Cellular Therapy, Institute of Medical Science, University of Tokyo, Tokyo, Japan), was cultured in Dulbecco's modified Eagle's medium (DMEM) (Nacalai Tesque, Kyoto, Japan) containing 10% heat-inactivated fetal bovine serum (GIBCO FBS; Invitrogen, Carlsbad, CA), 1% penicillin–streptomycin, and blasticidin (10 μg/ml). NIH3T3 cells were cultured in DMEM containing 10% heat-inactivated FBS and 1% penicillin–streptomycin. Vero/BC-F cells (a packaging cell line for hPIV2ΔF) (Ohtsuka *et al.*, manuscript in preparation) were cultured in modified Eagle's medium (MEM; Sigma-Aldrich, St. Louis, MO) containing 10% heat-inactivated FBS.

Generation of CD14-positive monocyte-derived DCs

Monocyte-derived dendritic cells (MoDCs) were generated as described previously with minor modifications (Elkord *et al.*, 2005). Peripheral blood was obtained from healthy adult volunteers with informed consent after approval by the Human Research Ethics Committee of the Mie University had been obtained (No. 2402). Peripheral blood mononuclear cells (PBMCs) were isolated by centrifugation with Ficoll-Paque PLUS (GE Healthcare Life Sciences, Piscataway, NJ). CD14-positive monocytes were purified from PBMCs by positive selection with CD14 microbeads (Miltenyi Biotec, Bergisch Gladbach, Germany). To generate immature MoDCs, CD14-positive cells were cultured in RPMI 1640 medium (Nacalai Tesque) containing 10% heat-inactivated FBS, 1% penicillin–streptomycin, 50 μ*M* 2-mercaptoethanol, and human granulocyte-macrophage colony-stimulating factor (GM-CSF) and interleukin (IL)-4 (each 50 ng/ml; both from Miltenyi Biotec) for 7 days at 37°C. Half the medium was replaced with fresh medium every 3 days. After 7 days, the purity of immature MoDCs (CD11c- and HLA-DR-positive cells) was >90% on flow cytometric analysis (data not shown).

Generation of bone marrow-derived DCs

Six- to 8-week-old female C57BL/6 and BALB/c mice were purchased from CLEA Japan (Tokyo, Japan). The animals were housed in a specific-pathogen-free condition facility in accordance with the guidelines of Mie University (Tsu, Japan). Bone marrow-derived dendritic cells (BMDCs) were generated as described previously with minor modifications (Inaba *et al.*, 1992). BM cells were isolated from the femurs and tibias of mice, and to eliminate red blood cells (RBCs) BM cells were incubated in RBC lysis buffer (phosphate-buffered saline [PBS] containing 150 m*M* NH_4Cl, 10 m*M* $KHCO_3$, and 100 μ*M* EDTA). After washing, BM cells were then cultured in RPMI 1640 medium containing 10% heat-inactivated FBS, 1% penicillin–streptomycin, 50 μ*M* 2-mercaptoethnol, and mouse GM-CSF and IL-4 (each 20 ng/ml; both from Miltenyi Biotec) for 7 days at 37°C. Half the medium was replaced with fresh medium every 2 days. After 7 days, the purity of immature BMDCs (CD11c-positive cells) was >80% on flow cytometric analysis (data not shown).

Preparation of hPIV2ΔF and retrovirus carrying the EGFP gene

Generation of the plasmid pEGFP-hPIV2ΔF and recovery of the hPIV2ΔF/EGFP viruses after transfection into Vero/BC-F cells were performed as described elsewhere (Ohtsuka *et al.*, manuscript in preparation). After 7 days, supernatant containing hPIV2ΔF/EGFP virus was recovered by centrifugation at 2000 rpm for 10 min, concentrated by ultracentrifugation at 28,000 rpm for 30 min at 4°C in a Beckman SW28 swinging bucket rotor with sterilized Beckman Ultra-Clear centrifuge tube (Beckman Coulter, Brea, CA), and then resuspended in PBS.

For inactivation of hPIV2ΔF/EGFP, β-propiolactone (BPL; Wako Pure Chemical Industries, Kyoto, Japan) was added to the purified supernatant at a final concentration of 0.05% (v/v) and incubated for 16 hr at 4°C. After incubation for 2 hr at 37°C, ultracentrifugation was then performed. Inactivation of hPIV2ΔF/EGFP was examined as follows: 1 ml of BPL-inactivated hPIV2ΔF/EGFP (BPL-hPIV2ΔF/EGFP) (1×10^6 plaque-forming units [PFU]) was added to 1 ml of medium of cultured Vero/BC-F cells, followed by incubation for 5 days, and 1 ml of culture supernatant was added to new